Review Vol. 16, No. 8 / 1 Aug 2025 / Biomedical Optics Express 3349
Biomedical Optics EXPRESS

Application of quantum imaging in biology

HODA LOTFIPOUR,[1] HASSAN SOBHANI,[1,*] MOHAMAD TAGHI DEJPASAND,[1] AND MORTEZA SASANI GHAMSARI[1,2]

[1] *Photonics and Quantum Technologies Research School, Nuclear Science and Technology Research Institute, Tehran, 11155-3486, Iran*
[2] *msasani@aeoi.org.ir*
[*] *hassan960sob@gmail.com*

Abstract: Application of quantum imaging in biology In biology, one of the main challenges is achieving a balance between high precision and minimal invasiveness in measurements. With cutting-edge techniques, the primary limitations to experimental accuracy often stem not from device-related noise but from fundamental physical constraints. Since nature is the underlying source of these constraints, it makes sense to go to quantum mechanics, the most basic theory of matter, for a solution. Improved measurement performance may be possible through the application of quantum effects, particularly those pertaining to coherence. It offers useful tools that, at the very least, offer interesting technical solutions even when they don't fully display cohesive behaviors. One of the primary applications of quantum technologies is quantum metrology, which uses the non-classical state of light to measure physical properties with great resolution and sensitivity. For biological applications, the quantum state of light may be utilized for precision enhancement and quantum noise reduction. This explains how quantum metrology, and particularly quantum imaging, can be used to enhance picture quality, measure shifts in quantum scales in biological systems, and boost imaging precision and resolution using quantum light sources, devices, and protocols. In this study, we give a summary of the possible uses of quantum technology in biology and medicine. This review presents a comprehensive overview of how quantum technologies can be applied in biology and medicine. It also explores the latest developments in quantum biological imaging, quantum microscopy, and quantum materials, while discussing the challenges and opportunities these emerging technologies bring.

© 2025 Optica Publishing Group under the terms of the Optica Open Access Publishing Agreement

1. Introduction

Biological systems serve as prime examples of complex systems. They often involve processes that are actively driven and accelerated by specific agents like enzymes, and display a wide range of emergent behaviors across different scales—from entire cells down to individual macromolecules and smaller. For these processes to occur, certain conditions such as concentration levels, temperature, pH, and other environmental factors must be precisely maintained. When studying these biological activities in real time, researchers face the challenge of achieving high measurement accuracy while minimizing disturbance to the system. This also includes accounting for how the measurement tools themselves might interfere with the system's normal operating conditions, not to mention their physical size. For instance, using intense light can increase the signal-to-noise ratio (SNR), but it might also heat the sample through absorption, potentially disrupting the process. This highlights the trade-off between maintaining non-invasiveness and achieving high precision. In the most advanced measurement methods, the main source of experimental uncertainty typically stems from fundamental physical limitations rather than from noise introduced by the instruments themselves [1]. In order to uncover biological processes occurring within living cells and organisms, imaging has been essential. Driven by intense curiosity, researchers have long tried to "see" biomolecules to verify their existence. Significant advancements in imaging technologies and instruments over the last

#566801 https://doi.org/10.1364/BOE.566801
Journal © 2025 Received 1 May 2025; revised 14 Jun 2025; accepted 18 Jun 2025; published 23 Jul 2025

Biomedical Optics EXPRESS

few decades have significantly increased our ability to study biomolecules' physicochemical characteristics, chemical and biological activities, and molecular behaviors up close. Our knowledge of numerous cellular activities has greatly increased thanks to these developments, which provide high spatiotemporal resolution and have made new discoveries possible [2]. Human physiology in both healthy and pathological conditions is now better understood thanks to recent advancements in biological imaging. Integrating these technologies with sophisticated mathematical models has shown great promise as they develop, but there are also many obstacles to overcome. Researchers can now link structural and functional data across different spatial and temporal scales by integrating imaging and modeling, which gives them a better understanding of fundamental biological systems and aids in clinical decision-making [3].

Advanced optical imaging techniques have been developed during the last 20 years to allow for high-speed and super-resolution bioimaging. Unfortunately, powerful light is usually needed to achieve high resolution and quick imaging, which might harm or interfere with the biological systems under study. Conversely, the use of low-intensity light frequently leads to a low signal-to-noise ratio because to stray light and shot noise. Quantum imaging techniques, which use correlated, entangled, or compressed photons, have been used by researchers to overcome the drawbacks of traditional optical imaging methods that rely on classical light sources [4]. Quantum imaging has a number of significant benefits over conventional optical imaging. First, even in low light, sub-shot-noise (SSN) imaging is possible because it can surpass the classical shot-noise limit. Secondly, it can lessen the effect of stray light. Thirdly, it enables imaging at super-resolution levels above the diffraction limit. Because of these advantages, quantum imaging is now a useful technique for researching biological specimens, which frequently have complex structures and are susceptible to damage from heat and photobleaching. Nevertheless, despite these benefits, low signal-to-noise ratios (SNRs) have thus far prevented quantum imaging of biological samples, mainly because of two key issues [5]. First, stringent conditions are needed to achieve SSN, like using detectors with high quantum efficiency or specimens with low absorption [6]. Second, the time constraints common to imaging procedures make it challenging to gather good coincidence rate data, which necessitates a high number of measurements. This frequently results in estimates of coincidence rates that are noisy or erroneous [7,8]. When considering the ratio of the field of view (FOV) to spatial resolution, most quantum imaging techniques still produce relatively low effective pixel counts—typically under 10,000—despite the availability of megapixel-scale widefield cameras [1,9]. Furthermore, the long data collecting durations of existing widefield systems make techniques like image tiling or stitching impracticable. Because of this, they are not appropriate for biological applications that call for the methodical imaging of several different areas within a single organism. Lastly, a complete and comprehensive measurement of birefringence properties utilizing quantum imaging has not yet been achieved, despite the fact that it can record transmittance and birefringence phase retardation [10,11].

In biological contexts, quantum imaging techniques enable the visualization of cellular structures and molecular interactions with extraordinary precision, potentially revealing dynamics that remain invisible to conventional imaging methods [7,12–14]. The non-invasive nature of many quantum imaging approaches makes them particularly valuable for studying delicate biological specimens in their native states.

Quantum microscopy integrates quantum light sources and detectors to achieve nanoscale spatial resolution and single-molecule sensitivity by exploiting quantum effects such as squeezed light states and quantum correlations, these advanced microscopic techniques push beyond the diffraction limit that constrains traditional optical microscopy. The resulting enhancement in both spatial and temporal resolution opens new avenues for investigating subcellular processes, protein folding dynamics, and the behavior of biomolecules at unprecedented scales [1,7,12,14,15].

Complementing these observational tools, quantum materials represent a class of engineered substances whose properties arise from quantum mechanical effects. When integrated with

Biomedical Optics EXPRESS

biological systems, these materials can serve as highly sensitive biosensors, targeted drug delivery vehicles, or interfaces between electronic devices and living tissues. Quantum dots, for instance, offer superior fluorescent properties for cellular labeling, while nitrogen-vacancy centers in diamond provide nanoscale magnetic resonance capabilities for probing biological environments [16,17]. Recently, several review papers have been published on quantum imaging [18–20]. Each of these papers discusses different aspects of recent progress in the field. However, there are several important points that need to be addressed in order to encompass all aspects of quantum biological imaging. This study aims to provide a new perspective, framework, and address the remaining challenges in quantum biological imaging. This paper explores the current state and future prospects of quantum imaging, quantum microscopy, and quantum materials in biological research, highlighting both the technical innovations driving this field forward and the fundamental quantum optical insights these approaches have already enabled.

2. Fundamentals

Compared to classical optical imaging approaches, quantum imaging is currently hindered by its slower speed and complicated setups. Nonetheless, the distinct benefits provided by entangled photon states enable quantum imaging for situations that are not enable to classical techniques. In particular, quantum imaging can operate with a very low light field by measuring the second-order correlation of entangled photons. The methods for detection successfully reduce uncorrelated background noise and accomplish sub-shot-noise imaging [18]. Quantum imaging benefits from the unique characteristics of entanglement. For instance, by using the nonlocality of quantum entanglement, polarization entanglement enables phase and dark-field imaging through nonlocal processes [18]. Consequently, becoming acquainted with the different quantum imaging techniques and platforms requires a comprehension of the foundations and principles of quantum optics. When necessary, a brief recap of fundamental ideas is given in this section.

2.1. Spontaneous parametric down-conversion

The phenomenon known as spatial entanglement occurs when particles that are geographically separated exhibit correlated wavefunctions associated with their spatial features. Typically, spontaneous parametric down-conversion (SPDC) is the process that creates this kind of entanglement. One high-energy photon is transformed into two lower-energy photons by a nonlinear crystal, causing SPDC [21]. A nonlinear crystal absorbs high-energy pump photons with specified momentum k_p and frequency ω_p in the SPDC process, releasing two lower-energy photons with identical momentum k_s and k_i and frequencies ω_s and ω_i. This mechanism conserves both momentum and energy, as indicated by the phase matching conditions $k_p = k_s + k_i$ and $\omega_p = \omega_s + \omega_i$ [22]. Beta barium borate (BBO), periodically poled potassium titanyl phosphate (PPKTP), and periodically poled lithium niobate (PPLN) are examples of nonlinear crystals that can be used to achieve high-dimensional entanglement and provide various forms of entanglement. Because of its wide frequency range, which spans from visible to infrared, BBO crystals are adaptable to a wide range of uses [23,24]. Different degrees of freedom, including polarization, momentum, and energy, can cause these pairings to become entangled [25–28]. In the bellow, a number of entanglements is maintained:

- Frequency entanglement:

If the frequency of pair photons which produced by the SPDC is entangled together the entanglement is frequency. The two-photon state produced by the SPDC for an incident undepleted CW pump may be written as Eq. (1):

$$|SPDC\rangle_\omega = |0_s\rangle|0_i\rangle + \gamma \int d\omega_s d\omega_i f(\omega_s, \omega_i)|\omega_s\rangle|\omega_i\rangle. \quad (1)$$

Biomedical Optics EXPRESS

where $|\omega_s\rangle$ and $|\omega_i\rangle$ are the states of the signal and idler, respectively and $f(\omega_s, \omega_i)$ is the joint spectral function (JSF). γ is proportional coefficient.

- Polarization entanglement:

Other kind of the entanglement is polarization entanglement. The EPR paradox was confirmed by Bell's test using entanglement in polarization [29,30]. Additionally, it is frequently utilized in quantum computing and communications because the vertical $|V\rangle$ and horizontal $|H\rangle$ states function as a discrete two-level system, enabling a short computing protocol [30–32]. It is possible to produce photon pairs with correlated polarizations from a single BBO crystal. When two BBO crystals are stacked with their optical axes perpendicular to one another, the source produces entangled photon states. For instance, the type-I SPDC state in BBO of the polarization applications is like Eq. (2):

$$|SPDC\rangle_{type-I} = \frac{1}{\sqrt{2}}(|H_s\rangle|H_i\rangle + |V_s\rangle|V_i\rangle). \tag{2}$$

One of the biggest challenges with BBO is phase matching, which requires precise angle tuning and temperature control. Through the use of quasi-phase matching, PPKTP and PPLN crystals enable effective SPDC over a larger range of wavelengths without the need for precise angle tuning. Higher stability and source power than BBO are offered by these crystals, which produce photons with high-dimensional entanglement. Nevertheless, when exposed to intense light, all three nonlinear crystals experience photorefractive degradation. For other instance, one of the type-II SPDC state can expressed as Eq. (3):

$$|SPDC\rangle_{type-II} = \frac{1}{\sqrt{2}}(|H_s\rangle|V_i\rangle + |V_s\rangle|H_i\rangle). \tag{3}$$

2.2. Interference with entangled photons

According to Abbe's theory, the wavelength of the photons involved affects spatial resolution. In coincidence measurements, the interference pattern can be used to infer the effective wavelength of bi-photons, which cannot be observed directly. Compared to classical imaging, quantum imaging exhibits an interference pattern twice as frequently. According to Milena D'Angelo [25], the term ' frequency' refers to spatial frequency. By employing entangled photon pairs in Young's double-slit experiment, D'Angelo et al. demonstrated that, under specific experimental conditions, the resulting two-photon interference-diffraction pattern exhibits a spatial modulation period that is half as large, and a diffraction width that is twice as narrow, compared to the classical case. The effective wavelength of bi-photons can be proposed to be half of the actual wavelength in photon pairs, given the proportional relationship between the interference pattern's frequency and the light source. Finer details in an image can be resolved more easily due to the greater frequency in the quantum interference pattern. If the double slits experiment is assumed to involve bi-photons and the biophotons propagate through a double slit to be considered, then the coincidence can be measured by two detectors, D1 and D2. The electric field at the detector D1 through the slit A and B is defined as $E_{A1} = u_0 e^{-ik\cdot r_{A1}}$ and $E_{B1} = u_0 e^{-ik\cdot r_{B1}}$. This allows for super-resolution when entangled photons are involved. Additionally, $E_{A2} = u_0 e^{-ik\cdot r_{A2}}$ and $E_{B2} = u_0 e^{-ik\cdot r_{B2}}$ are the definitions of the electric field at detector D2 through slits A and B. The amplitude of both photons' electric fields is denoted by u_0. The wavevectors associated with both slits can be reduced to the same value, $k_A = k_B = k$ since the double slits can be positioned symmetrically. The intensity of D1's classical interference is shown in Eq. (4):

$$\boldsymbol{G}_1^{(1)} = |\boldsymbol{E}_1|^2 = |\boldsymbol{E_{A1}} + \boldsymbol{E_{B1}}|^2 = 2\,|\boldsymbol{u}_0|^2\,(1 + \cos[\boldsymbol{k}\cdot(\boldsymbol{r_{B1}} - \boldsymbol{r_{A1}})]) \tag{4}$$

Biomedical Optics EXPRESS

In the same way, the interference intensity for detector D2 is like Eq. (5):

$$G_2^{(1)} = |E_2|^2 = |E_{A2} + E_{B2}|^2 = 2\,|u_0|^2\,(1 + \cos\,[k \cdot (r_{B2} - r_{A2})]) \tag{5}$$

The second-order correlation function, which represents the rate of coincidence measured by detectors D1 and D2 is expressed as Eq. (6):

$$G^{(2)} = 2\,|u_0|^2\,(1 + \cos\,[k \cdot (r_{B1} + r_{B2} - r_{A1} - r_{A2})]) \tag{6}$$

Phase $k{\cdot}r_{A1} = k{\cdot}r_{A2}$ and $k{\cdot}r_{B1} = k{\cdot}r_{B2}$ for entangled photons picked up by two detectors oriented symmetrically. The equation (6) deals with the joint detection probability of both entangled photons, leading to extremely distinct interference patterns. Furthermore, equation (6) contains a term which arises from the combination of four operator fields and represents the interference between the paths A→D1, B→D2 and B→D1, A→D2. This effect is due to two-photon interference and the non-classical nature of light, which is not observed in the classical model. Consequently, the interference pattern of the signal or idler photon is identical to the equation shown by $G^{(2)}$ in Eq. (7) [33]:

$$G^{(2)} = 2|u_0|^2(1 + \cos[2k \cdot (r_{B1} - r_{A1})]) \tag{7}$$

The spatial frequency of $G^{(2)}$ is twice that of $G_1^{(1)}$, indicating that the biphoton's effective wavelength is $\lambda/2$.

2.3. Spatial resolution of quantum imaging

In imaging, a diffraction pattern can be used in place of the two-photon interference pattern. Two entangled photons are assumed to travel through a single slit of infinitesimally small diameter d. For the photon signal, the classical diffraction field is provided at the position $r_s$by Eq. (8):

$$E_s = u_0 \sum_{k_s} e^{ik_s \cdot r_s} \tag{8}$$

All potential routes via the slit are indicated by the summing over the wavenumber k_s, which can be substituted by an integral over the slit area x in Eq. (9):

$$E_s = u_0 \int_{-d/2}^{+d/2} e^{ik_{s,\perp} x} e^{i\phi_s} dx, \tag{9}$$

where φ_s is the signal photon's propagation phase and $k_{s,\perp}$ is the wavevector's projection on the slit plane. The essential comes back in Eq. (10):

$$E_s = u_0 d\,\mathbf{sin}c\left(\frac{k_{s,\perp} d}{2}\right) e^{i\phi_s} \tag{10}$$

Therefore, the diffraction pattern is like Eq. (11):

$$G_s^{(1)} = u_0^2 d^2\,\mathbf{sin}c^2\left(\frac{k_{s,\perp} d}{2}\right) \tag{11}$$

A slit's diffraction pattern can be used to assess the resolution in a conventional imaging system. The spatial resolution has an impact on the central maximum's bandwidth. We may now

Biomedical Optics EXPRESS

detect the entangled photons at the same time. The signal and idler photons' quantized electric fields are as Eq. (12) and Eq. (13):

$$E_s^{(+)} = u_0 \sum_{k_s} a_{k_s} e^{ik_s \cdot r_s} \tag{12}$$

$$E_i^{(+)} = u_0 \sum_{k_i} a_{k_i} e^{ik_i \cdot r_i} \tag{13}$$

Since the wavevectors k_s and k_i are related, we only have to sum over k_s. The two photons' correlation can be clearly shown by using the identical phases, $k_s \cdot r_s = k_i \cdot r_i$ as Eq. (14):

$$G^{(2)} = |u_0|^2 \left| \sum_{k_s} e^{ik_s \cdot r_s} e^{ik_i \cdot r_i} \right|^2 = |u_0|^2 \left| \sum_{k_s} e^{i2k_s \cdot r_s} \right|^2 \tag{14}$$

To demonstrate that the final expression of $G^{(2)}$ is comparable to that of $G_s^{(1)}$, we can repeat the computations above to reach Eq. (15):

$$G^{(2)} = u_0^2 d^2 \mathbf{sin}c^2(k_{s,\perp} d) \tag{15}$$

The core pattern's bandwidth is half of $G_s^{(1)}$. In terms of spatial performance, bi-photons can be thought of as one with a half wavelength or a twofold spatial frequency due to the correlation between the phases of entangled photons. Because of this, the biphoton resolution reaches super-resolution at the Heisenberg limit in contrast to the signal or idler photon.

2.4. Some important terms

The location of the detector is very important in quantum imaging, especially for methods like ghost imaging, where the image quality is significantly impacted by the detector orientation. Depending on the particular imaging method, the relative locations of the detectors may affect the resolution and picture generation process. For instance, both detectors may be situated in the down-conversion crystal's picture plane in certain arrangements. Some of the concepts and quantities that will be introduced in order to improve both of them need to be defined here. In quantum imaging, "terms" relate to the particular ideas that are used to explain the physics and procedures that are involved. The point spread function (PSF) is the initial term in quantum imaging. The PSF measures a detector's ability to discriminate between two ideal spots that are spaced apart. Let us assume that imaging equipment with a huge number of pixels records an image of a perfect point. These pixels can be thought of as distinct detectors that are spaced apart by a tiny amount of pitch or distance. The image will have a spherical shape with the highest intensity in the center and rapidly diminishing intensity as one moves away from the center if the radiation utilized to form the spot image on these pixels is monochromatic and perpendicular to both surfaces [34].

This intensity can now be plotted against any single coordinate to produce a Gaussian-like distribution (the image will be radially symmetric for a perfect point). We call this distribution one-dimensional. It goes without saying that the distribution is never entirely Gaussian and may even be skewed. We can still define a quantity known as full width at half maximum, or FWHM, so for the most part, it doesn't really matter how it looks. Clearly, the detector will be able to detect one spot from the other if the distance between them is equal to or more than FWHM. Consequently, the value of FWHM determines the system's spatial representation in Eq. (16).

$$f(x) = \frac{1}{\sqrt{2\pi\sigma^2}} \exp\left[\frac{-(x - x_0)^2}{2\sigma^2}\right] \tag{16}$$

where σ is the standard deviation and x_0 is the function's center. This function's FWHM is provided by; FWHM$\approx 2{\cdot}36\sigma$. The second key concept is the line spread function (LSF), which is

Biomedical Optics EXPRESS

comparable to PSF in that it measures spatial resolution using the same methodology. But in this instance, a point is substituted with the picture of an ideal line. Next, through this image, the LSF is drawn perpendicularly. The LSF generates a whole profile of FWHMs rather than a single value, like the PSF does, because a line may be conceived of as being made up of several closely spaced points. This profile can then be used to determine the system's resolution at any given time. Despite being a useful indicator of system resolution, LSF is extremely challenging to quantify experimentally. The third key concept in quantum imaging is the edge spread function. Because of the engineering challenge of designing an ideal line object, the LSF does not provide a very useful way to determine system resolution. In this context, the edge spread function (ESF) is more practical since it considers the image of an ideal step function, which is readily obtainable from a rectangular object. The integral of one-dimensional PSFs can be used to define the ESF, which is show in Eq. (17) and 18 [35]:

$$ESF(x) = \int LSF(x)dx \tag{17}$$

or

$$LSF(x) = \frac{d}{dx}[ESF(x)] \tag{18}$$

To understand the role of these terms in evaluating the experimental results, we consider an example. As an example, the approach taken by Zhang et al [5] can be introduced. In their study, they aimed to measure the spatial resolution of a quantum imaging system by extracting the profile of a line along the x-axis, which is perpendicular to an edge in the USAF resolution target. They fitted this profile to an edge spread function (ESF) centered at x_0, represented by the equation; $ESF(x) = a \times erf((x - x_0)/w) + b$, where a and b are coefficients, and w represents the radius of the beam. A Gaussian LSF was obtained by taking the derivative of the ESF, i.e., $LSF(x) = dESF(x) / dx = 2a \times exp(-(x - x_0)^2 / w^2) / (w\sqrt{\pi})$. In their experiment, the resolution was estimated to be the FWHM of the LSF, i.e., $\mathcal{R} = 2\sqrt{ln2}w$. The mean value of the resolution was estimated to be $2\sqrt{}$ ln2w. ln2 times the fitted w, and the SE was calculated to be ln2/1·96 times the 95% confidence interval of the fitted w.

Furthermore, as this study is about quantum imaging, it is necessary to introduce and discuss important metrics like contrast and signal-to-noise ratio (SNR) appropriately. The signal-to-noise ratio (SNR) in quantum imaging is the ratio of the signal strength to the background noise level. A greater SNR denotes a higher-quality image with details that are easier to see. It basically measures how well the signal of interest can be distinguished from unimportant noise. Since the corresponding signal-to-noise ratio (SNR) is proportional to the square root of the intensity, $\sqrt{I}$, increasing the light intensity utilized for the measurement can improve the SNR. The high intensity at incidence, however, can result in undesired photo-sensitive effects or optical damage, so raising the optical power is not always appropriate [36]. Using quantum probes to take advantage of the advantageous quantum features of light that are not present in classical probes has been proposed as an alternate method of reaching a targeted SNR in such constrained settings, rather than raising the optical intensity [36]. For different imaging processes, the SNR definition varies [37,38]. A ghost imaging protocol's signal-to-noise ratio, for instance, is the ratio of the mean "contrast" to its standard deviation (mean fluctuation) as Eq. (19) [37]:

$$SNR_s = \frac{|\langle S_{in} - S_{out}\rangle|}{\sqrt{\langle \delta^2(S_{in} - S_{out})\rangle}} \tag{19}$$

where S_{in} and S_{out} are the intensity values of the reconstructed ghost image, and $\delta S \equiv S - \langle S\rangle$ is the fluctuation. The mean value, denoted by $\langle\ \rangle$, represents the theoretical expectation value, which can be estimated in practice by performing space averages over the regions "in" and

Biomedical Optics EXPRESS

"out" of the ghost image. The ghost image can be reconstructed by exploiting different GI protocols, namely, different parameters S [37]. Lupo [38], have reported that for a Gaussian point-spread function the signal-to-noise ratio, $SNR = \eta N/\varepsilon$, N is the mean photon number, η is the transmissivity of beam splitter and ε is the variance of Gaussian random variables. Erkmen and Shapiro [39], determined the signal-to-noise ratios (SNRs) of three Gaussian-state ghost imaging setups depending on the type of light source applied. They employed two distinct classical-state light states, namely a joint signal-reference field state with a correct P representation, that have either the greatest phase-insensitive or the maximum phase-sensitive cross correlation. An entangled signal-reference field state with the maximum phase-sensitive cross correlation permitted by quantum physics is the third method they employ, which makes use of nonclassical light. We develop analytical SNR equations and give simple asymptotic approximations for both low- and high-brightness sources in the near-field and far-field regimes. An SNR is usually larger for a high-brightness thermal-state (classical phase-insensitive state) source than for a biphoton-state (low-brightness, low-flux limit of the entangled-state) source [39].

3. Quantum optical imaging

Quantum metrology, one of the main fields of quantum technologies, utilizes the quantum properties of light (such as quantum coherence and correlations) to improve resolution and measurement. One unique field within quantum metrology is quantum optical imaging [8,40], which offers several advantages compared to classical optical imaging. These advantages include noise reduction [8,41], resolution enhancement [5], precision improvement, surpassing the diffraction limit [42,43], and exceeding the shot noise limit. This technique uses low-intensity illumination, making it suitable for photosensitive specimens like biological samples [1,5,15, 44]. In these samples, photo-bleaching, thermal damage, and optical damage can occur at high optical intensities [44]. Fig. 1 shows various schemes for quantum optical imaging, which will be discussed in later sections. In this section, we investigate recent progress in quantum optical imaging with biological applications.

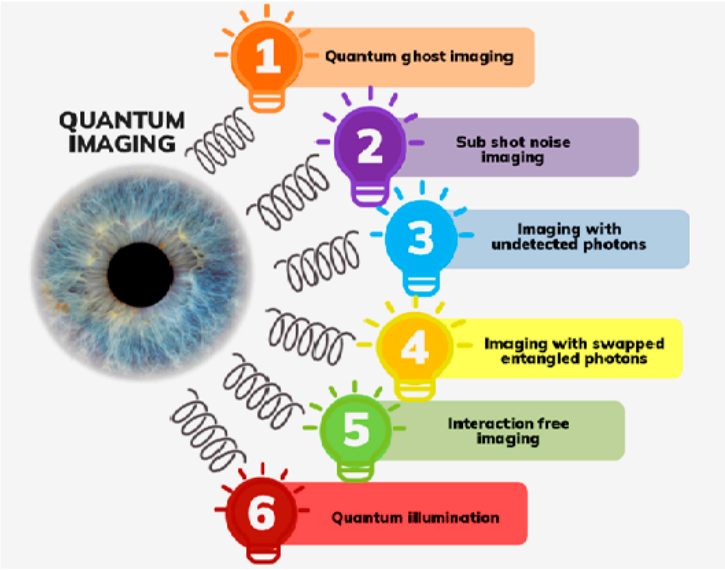


Fig. 1. Various quantum imaging schemes [45].

Biomedical Optics EXPRESS

3.1. Quantum ghost imaging

Quantum ghost imaging (QGI) is a quantum correlation-based technique that records images using photons that have not interacted with the object [46]. This technique uses quantum entangled photons as spatially correlated light generated in the SPDC process. The idler photons interact with the object and are detected by a bucket detector, which is not spatially resolved. One of the earliest experimental realizations of this phenomenon was reported by Pittman et al. [47], who demonstrated that an image could be reconstructed through spatial correlations between entangled photon pairs, even though the imaging photon had no direct interaction with the object. Meanwhile, the coincidence detection of signal photons via an imaging detector and the idler photons generates the image [48]. The idler photons that pass through the sample are detected with a non-spatially resolving detector. This detector only indicates when a photon arrives and does not include spatial information. On the other side, the signal photons do not interact with the sample but are detected with a spatially resolved, less noisy, and more sensitive detector that measures the position of all the signal photons. The correlation between the two series of data from the detectors can be used to extract an image. By integrating over a number of acquired events, an image of the object can be recovered from the subset of the signal light field that is correlated with the idler light field detected by the bucket detector. In this technique, each field alone does not carry complete information, but their correlation is used to reconstruct the image. Originally, quantum ghost imaging was a result of quantum entanglement in an SPDC process. The main advantage of QGI compared to its classical counterpart is the use of quantum light, resulting in higher visibility and a greater signal to noise ratios (SNRs) [49,37] in low-intensity light conditions. Since this method uses a low photon flux interacting with the sample, resulting in low photodamage, QGI is beneficial for sensitive structures such as biological matter [33]. Digital quantum ghost imaging utilizes digital objects for biological samples. In ghost imaging, non-degenerate signal and idler photons generated via the SPDC process can be used when the biological sample is illuminated with one wavelength, such as mid-infrared, which is suitable for probing biological samples. The image is then reconstructed with another wavelength to reduce photodamage in sensitive samples [50].

In 2015, Morris et al. [50] suggested a new technique (time-gated imaging system) in ghost imaging based on a multi-array detector, while previously, a resolved single-pixel detector had been used. Using heralded single photons enables counting the number of single photons in the image. They recorded an image of a wasp wing with a low photon number, where the average photon-per-pixel ratio was less than one (0·45). The natural sparsity in the spatial frequency domain and the Poissonian statistics of data were utilized to improve image quality.

Losero et al. [13] demonstrated quantum differential ghost imaging (QDGI) using quantum correlations via a low-brightness SPDC source and non-classical intensity correlation-based imaging. Compared to conventional QGI, this method improves the SNR at a fixed exposure time using a quantum source (SPDC) without increasing the photon dose for transparent samples. The imaging occurred in the low-intensity regime, where the number of photons per pixel was 10^3. In this regime, the reconstruction of images is based on intensity correlations and does not require time-coincidence. This method is applicable for biological, delicate, or photosensitive samples. Two biological samples were imaged: a Polistes wasp wing and a green bug wing. Fig. 2 shows the experimental scheme of QDGI.

3.2. Sub-shot noise imaging

One of the most important aspects of quantum-enhanced sensitivity is using quantum light with a small number of photons for imaging delicate systems in biochemistry, biology, and medicine. Low-intensity light does not affect sensitive biological samples as an environmental stress. One of the simplest, fastest, and least expensive classical imaging techniques used in live biological systems is wide-field microscopy. Sub-shot-noise quantum imaging (SSNQI) employs

Biomedical Optics EXPRESS

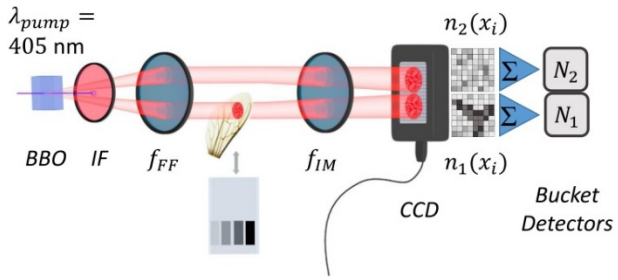


Fig. 2. The experimental scheme of quantum differential ghost imaging (QDGI) [13].

quantum-correlated beams to enhance resolution and sensitivity. In this method, one beam interacts with the sample while the other serves as a reference. The theory of this technique was investigated by Brida et al. in 2010 [52]. The first experimental implementation of a wide-field subshot-noise limit (SNL) microscope was reported in 2017 [53]. In this method, images consist of 10^4 pixels and have a spatial resolution of a few micrometers. In 2020, Berchera et al. [54] demonstrated simultaneous improvement in resolution and sensitivity gain their classical counterparts. The multi-mode twin-beam state was generated through the SPDC process. The output state was approximated as a tensor product of independent two-mode squeezed vacuum states where the momentum and wavelength of interacting photons were correlated.

3.3. *Imaging with undetected photons*

Quantum imaging with undetected photons (QIUP) is an induced coherence-based imaging technique, first introduced by Zou, Wang, and Mandel [55]. In this method, there is no need to detect the idler photon. By using two nonlinear crystals in a nonlinear interferometer, a pair of signal and idler photons is generated by the SPDC process in the first crystal. The idler photons interact with the biological sample and enter the second nonlinear crystal, inducing coherence between the two signal beams. The pump laser, initially split into two parts by a beam splitter, enters the first crystal with one part, while the other part is co-axially aligned with the interacting idler and enters the second nonlinear crystal. The signal beam output from the first and second crystals enters a beam splitter and produces an image at its output. The two signal beams interfere via the beam splitter. Although these beams do not interact with the sample, the phase and transmission properties of the sample affect their interference. The physical phenomenon that occurs in the nonlinear interferometer is based on the superposition of two idler beams, as it is unclear which crystal generates the idler. This induces bi-photon coherence in the generated photon pairs. The signals combined in the beam splitter are not known to originate from either crystal. The indistinguishability between the pair of signals and the idler produced by the first and second crystal is required to cause interference with high visibility. When the sample enters the idler path between two crystals, the degree of indistinguishability is reduced, and the coherence and visibility of interference decrease [56,57]. One advantage of this method is that imaging and interaction can be done at different wavelengths [58]. This makes it useful for biological imaging where the interaction wavelength is in the near-IR range, but the imaging is in the visible wavelength. This method can also be applied to spectroscopy for biological samples in the infrared range [59].

An important consideration in using QIUP for biological applications is spatial resolution. The resolution required in biological imaging is about a few microns or lower. Zeilinger et al. [60] imaged a zebrafish embryo with sub-mm feature size using this method. In 2020, Buzas et al. [61] sought to increase the spatial resolution in infrared microscopy of biological samples (wing of a garden fruit fly and NIES-39 spirulina strain) in an experimental setup. They improved the

Biomedical Optics EXPRESS

spatial resolution by an order of magnitude (reported as 2 microns) compared to other methods using quantum imaging with undetected photons. Previously, a resolution of 15-20 microns was reported [50,51,58,60] in quantum imaging. To break the Rayleigh limit for spatial resolution, scanning-assisted imaging is utilized in quantum imaging methods. Fig. 3 shows the schematic representation of scanning interference microscopy with undetected photons setup and images of biological samples at different step sizes. For better efficiency in biological applications, the nonlinear crystal type is chosen so that the wavelength of the idler photons (1345 nm) that interact with the biological sample is in the infrared region and far from the absorption wavelength of water. Meanwhile, the wavelength of the signal photons (880 nm) to be detected is located in the better performance range of CCD cameras.

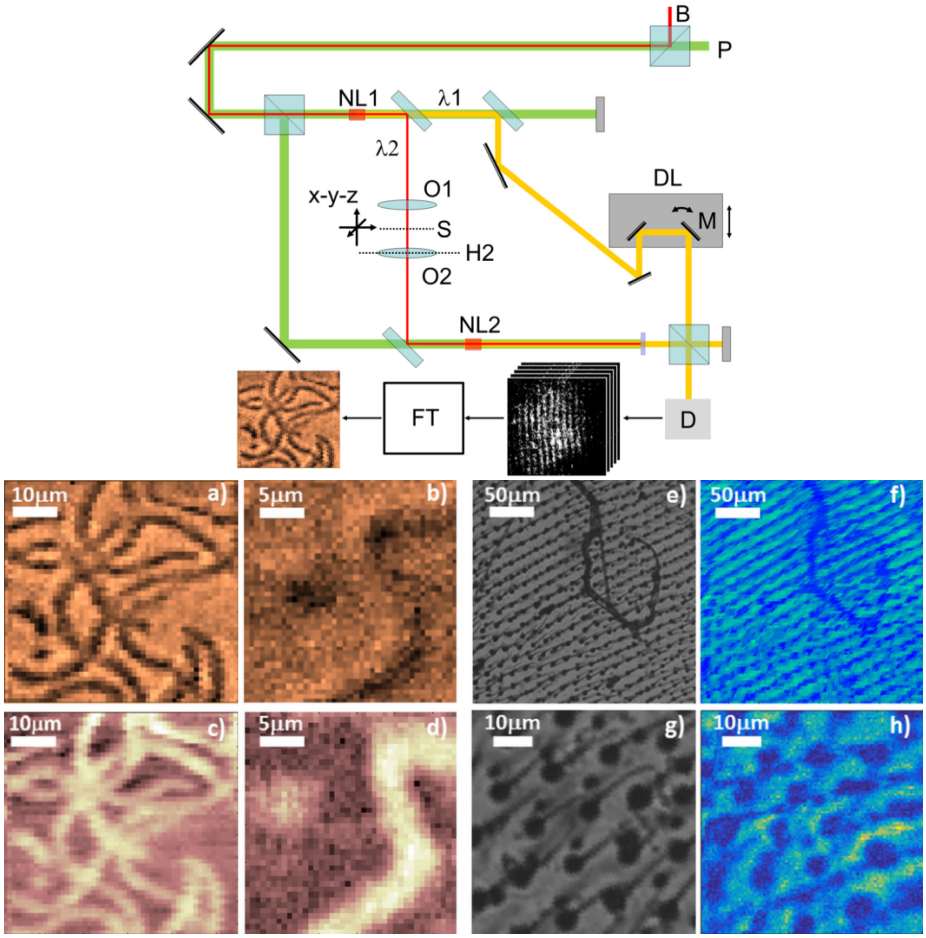


Fig. 3. Schematic representation of the experimental set-up and the images of biological samples (a-d): Spirulina filaments and (e-h): fruit fly wing at different scan areas and step size [61].

3.4. *Interaction-free measurement*

In this imaging method, the sample does not interact with the signal or idler beam, but object information can be obtained via imaging [62]. Although probe photons in both QGI and QIUP interact with the sample, in interaction-free imaging, supersensitive object information can be obtained without requiring direct interaction. This method uses a Mach-Zehnder interferometer

Biomedical Optics EXPRESS

with two detectors to record the constructive or destructive pattern of interference. If the interferometer is balanced and the two paths are indistinguishable when a single photon enters the setup, constructive interference occurs. However, when a sample is placed in one arm of the interferometer, the path becomes distinguishable, and the wave-particle duality of single photons causes the photons to behave like individual particles, resulting in destructive interference.

This method utilizes the induced coherence phenomena in the interferometer. Although the idler photons do not interact with the object, they carry the sample information and transfer it to the signal photons using induced coherence. The image can be reconstructed by a visible range signal-photon detector with no spatial resolution [63–65]. In 2023, Yang et al. [66] demonstrated interaction-free, single-pixel quantum imaging with undetected photons. They used a single-photon Michelson interferometer with double-pass SPDC processes, which play the roles of sources 1 and 2 in Fig. 4. They combined induced coherence (IC), interaction-free measurement (IFM), and single-pixel imaging (SPI) in the experimental setup (Fig. 4). Three different arms are placed in the interferometer, indicated with circled numbers. The idler beam is blocked for the undetected part of the method using dichroic mirror DM3. In this setup, the generated photons and the detected photons have not interacted with the sample, making this method potentially useful for photosensitive systems such as biological applications. They also suggested that utilizing single-photon detectors in visible wavelengths is more economical and offers low-noise, high-efficiency capabilities. In recent years, some schemes have been suggested for combining interaction-free imaging and correlation-based quantum imaging to improve resolution, contrast, and precision, which have potential for imaging photosensitive biological tissues [13,42,43].

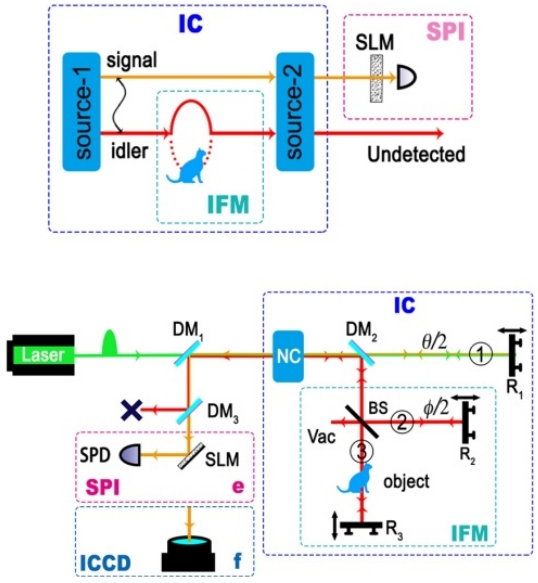


Fig. 4. three physical phenomena (induced coherence (IC), the interaction-free measurement (IFM), single-pixel imaging (SPI)) in the schematic setup (top)- The experimental setup of interaction-free, single-pixel QIUP (Down) [66].

3.5. *Imaging with entangled photons*

There are several challenges in quantum imaging for biological applications, such as low SNRs, low resolvable pixel counts, difficulty in imaging biological organisms, and inability to quantify full birefringence properties. Entanglement-based imaging (EBI) can be utilized to overcome

Biomedical Optics EXPRESS

these challenges. In 2024, Zhang et al. [5] demonstrated that using spatially entangled photons and their coincidence can improve SNRs and resolvable pixel counts to facilitate high-quality imaging of biological organisms. They utilized the "entanglement pinhole effect" by simultaneously using two detectors to create quantum images of mouse brain slices and zebrafish with a field of view up to 7 mm × 4 mm. They also exploited polarized entangled photons for quantum birefringence imaging to remotely recognize birefringence properties without changing the polarization states of the photons incident on the object. One unique advantage of this method is the remote sensing of full birefringence properties, which cannot be achieved using classical methods. Although utilizing multimode SPDC photons leads to an increase in the spatial mode in each pixel, it results in reduced spatial resolution compared to the Abbe limit of resolution. Using a high-intensity entangled photon source improves the SNR and imaging speed. In this method, the optical power illuminating the specimen Is about $4{\cdot}9 \times 10^{-15}$ W, which is suitable for photosensitive biological specimens. Fig. 5 shows the experimental setup of EBI [5].

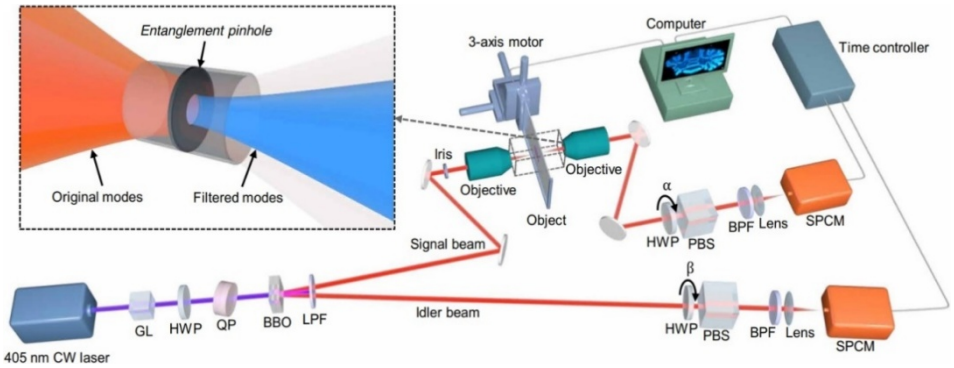


Fig. 5. The schematic experimental setup of imaging with entangled photons [5].

In 2021, quantum holography of biological specimens (bird feathers) was introduced using spatial-polarization hyper-entangled photons, and phase images of sensitive objects were reconstructed [7]. The phase image information is encoded into the polarization property of entangled photons, which is represented by the intensity correlation of photon pairs via coincidence count. This method can be exploited in exploring birefringence variation of biological specimens such as cell pathophysiology, tissue damage, and ophthalmologic preclinical diagnosis, where classical methods do not work due to phase disordering and the presence of stray light. The basic advantages of this method are remote interferences between reference and illuminating photons with no need for path overlap, robustness against dephasing decoherence, resistance to classical noise, and improvement of spatial resolution by a factor of 1·84 [7]. To provide a clearer understanding of the advantages, limitations, and suitability of different quantum imaging approaches in biological contexts, we present a comparative table (Table 1). This summary includes key performance indicators such as resolution, type of quantum light used, potential biological applications, and references to representative studies. The comparison aims to guide researchers in selecting appropriate techniques for specific bioimaging needs, particularly where sensitivity, resolution, and sample preservation are critical.

Biomedical Optics EXPRESS

Table 1. Comparative overview of major quantum imaging techniques applied to biological systems.

Imaging Technique	Approx. Resolution	Contrast	Advantages	Limitations	Biological Application	Significant Parameter
Quantum Light Source		SNR				
Ghost Imaging	Sub-mm		Low-light, non-invasive, high SNR	Low speed, needs temporal correlation	Wasp wing, insect samples	Number of Photons per pixel=10^3
Entangled photons [13]		1-5				
Ghost Imaging	~100 µm	≈ 0.7	No interaction with object, low photon flux required, clear image formation	Reduced trigger rate due to object attenuation; requires ICCD and delay line	Wasp wing imaging with <0.5 photon/pixel	FOV: 4×4 mm^2 Acquisition time per resolvable pixel (s):0.7 Resolvable pixel count::2401
SPDC (Entangled photons) [50]		6				
Sub-shot-noise Imaging	Few µm		Ultra-low noise, suitable for live samples	Sensitive to loss, needs precise alignment	Live cell imaging	acquisition time of a single frame is 100 ms noise reduction factor (NRF)=0.3-0.8
Quantum-correlated beams [54]						
Imaging with Undetected Photons	2 µm	maximal visibility: 0:62 ± 0:05	Dual-wavelength interaction and detection	Complex setup with dual crystals	Fruit fly wing, Spirulina	
Entangled photon pairs (idler undetected) [61]						
Interaction-Free Imaging=0.4	width of the edge:43 µm	Visibility: *≈93.9%*	No direct sample contact, ideal for sensitive systems	Complex interferometry	Photosensitive structures	mean counts per second: 3,500 and 2,950
Single photons (no direct interaction) [66]						
Imaging with Entangled Photons	Few µm (13.3-78.4 µm)		High SNR, birefringence sensing	Photon flux limitations, resolution tradeoff	Mouse brain, Zebrafish	Acquisition time per resolvable pixel (s)=1 Resolvable pixel count: Up to 258,432 FOV: Up to 7×4 mm^2
Entangled photons [42]		40				
Quantum Microscopy	1.4 µm Max spatial resolution:8	Max Contrast to noise ratio(CNR):8	super-resolution microscopywith up to 5 times higher speeds, twofold resolution improvement, 2.6 times higher CNRs, and 10 times more resistance to stray light than existing wide-field quantum imaging techniques	Still low speed, complex hardware	Cell dynamics, deep tissue, cancer cells	
Entangled photons [15]						
Quantum Holography	~λ/2		Phase imaging, robust to dephasing	Requires coincidence detection	Bird Feather, cellular birefringence	FOV: 2×1 mm^2 Resolvable pixel count:968 Acquisition time per resolvable pixel (s):63
Polarization-entangled photons [7]		13				

Biomedical Optics EXPRESS

4. Quantum microscopy

Classical microscopic imaging use high-intensity light, which can destroy a sample. Furthermore, classical imaging techniques are fundamentally limited by the limits of diffraction and shot noise, limiting their ability to resolve fine details and detect weak signals. Quantum microscopy aims to overcome these limitations by exploiting the unique properties of quantum states of light.

However, the development of wide-field quantum imaging has serious obstacles such as low spatial resolution, low speed, and low contrast-to-noise ratio. Recently, a quantum microscopy is proposed by employing coincidence with balanced path-lengths. The scheme can achieve a super-resolution imaging at the Heisenberg limit with substantially higher speeds and contrast-to-noise ratios than existing wide-field quantum imaging methods [15]. In the quantum microscopy by coincidence with balanced path-lengths resists stray light up to 155 times stronger than classical signals which is experimentally and theoretically proved [15]. Quantum-correlated photons can allow the minimum microscope noise to drop below the typical shot noise limit due to the randomness of the photon statistics [1,67]. This can cause the microscope to scan at a lower light intensity or at a higher speed. Similarly, the fact that a fluorescent indicator can emit only one photon at a time, together with accurate photon counting, provides information that enables new types of super-resolution microscopes [68]. Entangled photons can allow the microscope to be exploited at wavelengths that are difficult to scan, such as the mid-infrared [14,69]. The microscopy in mid-IR can provide a powerful tool for better imaging. The imaging over a broad wavelength range covering 3·4 to 4·3 μm by a resolution of 35 μm is demonstrated [13]. Several types of quantum correlation have been used to increase the SNR in microscopes. The quantum correlation between photons can reduce the variance of the optical noise or to increase the signal strength to improve the SNR.

By using the Hong-Ou-Mandel (HOM) effect, the implementation of super-resolution microscopy with two-photon interference has been reported. The sensitivity of the microscope is controlled by the wavelength separation between the two photons if entangled pairs. In the research, the axial precision is reported using up to 12·3 nm of detuning and ~ 104 detected photons pairs [70]. So, the microscope based on the HOM interferometry, reach higher Fisher information per photon, which can be an important consideration for photo-sensitive samples and can otherwise be a limiting factor for measurement precision [71]. The possibility of HOM microscopy as a tool for label-free imaging of transparent samples is demonstrates by investigating the bunched and anti-bunched photon-pair distributions at the HOM interferometer output [72]. A reduction of noise in a coherent mode due to Kerr squeezing with a photonic crystal fiber is used to increase the precision in absorption microscopy. The classical noise is reduced by taking fast measurements and modulating the probe in time to be in a shot-noise limited bandwidth of the detector and the laser. The shot-noise precision on single-pixel measurements with squeezing of Φlog = -0·88 dB for ~ 200 μW of light detected is reported.

Among the applications of optical phase measurement, interference-based microscopes are widely used to evaluate opaque materials or biological tissues. However, the SNR for a given light intensity is limited by the standard quantum limit (SQL), which is critical for measurements where the light intensity has the potential to damage the sample.

The standard quantum limit can only be beaten by using N quantum correlated particles, with an improvement factor of $\sqrt{N}$. Recently, a microscope based on the entanglement, which is a confocal-type differential interference contrast microscope where an entangled photon pair source is used is reported. In the report, the SNR is 1·35±0·12 times better than that limited by the standard quantum limit [73]. By applying the intensity correlation between spatially correlated beams of light, a confocal microscope is demonstrated [74]. Furthermore, the authors in new report, a two-channel confocal microscope are proposed which offers further resolution enhancement [75]. All types of classical microscopes that have been built rely on classical light sources that are noisy due to the random timing and location of the detected photons. Recently, a

Biomedical Optics EXPRESS

two-beam optical microscope using a non-classical light source consisting of entangled photon pairs produced by a nonlinear optical parametric transformation process has been proposed. Entangled sources have been employed to imaging techniques such as ghost imaging, quantum holography, and quantum optical coherence tomography. A new method for imaging with super-resolution is proposed as quantum image scanning microscopy. This method generates a robust resolution enhancement without sacrificing the signal level. By employing the measurement of quantum photon correlation, the resolution of image is raised up to two-fold, four times beyond the diffraction limit [12]. In the method, to achieve the super-resolved optical images of a biological sample stained with fluorescent quantum dots [12]. A powerful label-free imaging method that can probe the vibrational response of chemicals of polymers and biological samples, with high sensitivity is quantum stimulated Raman scattering microscopy. By employing the squeezed state, the microscope can operate below the shot noise limit, increasing the performance without increasing the illumination intensity.

The quantum stimulated Raman scattering microscope, operating at the optimal efficiency, is applied to biological samples. The imaging speed of 100×100 pixels in 18 seconds allows the dynamics of cell organelles to be resolved. The quantum stimulated Raman scattering microscope yields a 20% improvement in imaging speed compared to shot noise limited operation [76]. Furthermore, a coherent Raman microscope with a 35 per cent improved SNR compared with conventional microscopy corresponding to a 14 per cent improvement in concentration sensitivity is demonstrated [78]. Furthermore, the squeezed state also has been applied in a Raman microscopy [77]. To determine both axial and lateral positions of individual fluorophores with nanometer accuracy, a stochastic optical reconstruction microscopy is demonstrated. By stochastic optical reconstruction microscopy, an image resolution of 20 to 30 nanometers in the lateral dimensions and 50 to 60 nanometers in the axial dimension has been achieved [78]. Because the two-photon absorption is related to the third-order nonlinear effect, it occurs only near the central focus of illumination. By comparing two-photon absorption with single-photon absorption, it can be seen that not only is the spatial resolution sharper in two-photon absorption, but it also suppresses the fluorescence from the focal plane. Furthermore, to increase efficiency in two-photon absorption, we need the quantum correlations instead of high-peak-intensity pulsed lasers which can damage the specimen. One of classical microscopy which use two-photon absorption is two-photon absorption microscopy. The two-photon absorption is a nonlinear process in which two photons are required to bridge the energy gap between the ground and excited states. These phenomena require high-power lasers with short pulses to overcome the low absorption efficiency (low two-photon cross sections). The first advantage of two-photon absorption microscopy is that it provides a higher the SNR compared to single-photon absorption techniques. If the two photons involved in the two-photon absorption process were entangled, it provides a higher the SNR compared to classical two-photon absorption [79]. Compared to single-photon absorption, two-photon absorption not only improves spatial resolution, but also suppresses fluorescence from the focal plane [44]. Furthermore, without quantum correlations, two-photon absorption is an inefficient phenomenon, that requires a high-intensity pulsed lasers, which can damage the sample [44].

There are several techniques to experimentally generate entangled photon pairs, but the most popular is through the SPDC. In this process, coupled photons are produced simultaneously, in other words, they have time-correlation and energy anti-correlation. The energy correlation are used for microscopes applications [79]. Entangled photon pairs are used instead of correlated classical light to increase the absorption rate. The enhancement of absorption, allows multi-photon fluorescence microscopy. So the required entangled photon flux is comparable to similar classical coherent photons, allowing a 10 order of magnitude reduction in power from tens of mW to a few pW [80,81]. So, an entangled microscope illuminate with a NOON state is better than the entangled photons generated by the SPDC process to have superior resolution [82]. The

Biomedical Optics EXPRESS

entangled microscope illuminate with a NOON is produced by combining a laser by coherent state with a pair- photons generated by the SPDC crystal. By the configuration, the sensitivity of the phase images is improved close to the Heisenberg limit [83]. Furthermore, the NOON states have been successfully integrated into phase-contrast microscopes [83]. Furthermore, the squeezed state also has been applied in a probe scanning microscopy [84] and stimulated emission microscopy [85].

5. Quantum optical measurement techniques in support of quantum imaging

Quantum imaging in biology does not only rely on image formation, but also requires very precise measurements of the optical parameters of the sample. To achieve high resolution and sensitivity in such complex environments, classical imaging methods alone are not sufficient. In fact, many advanced quantum imaging techniques are directly or indirectly based on precise quantum measurements of the optical properties of the sample. For this reason, the use of quantum optical measurement techniques is not only complementary to quantum imaging, but in many cases a prerequisite for its realization.

Quantum measurement is an advanced branch of physical metrology that exploits nonclassical properties of light—such as entanglement, quantum compression, discrete photon states, and quantum interference—to provide significant improvements in accuracy, sensitivity, and resolution over traditional methods. Unlike classical measurements, which are inherently affected by shot noise and statistical limitations, quantum measurement overcomes these limitations by designing specific optical modes and appropriate detectors. In biology, where samples are often light-sensitive, in aqueous, and highly scattering environments, the use of high-power light sources can destroy or alter the natural behavior of the system. Quantum measurement offers a smart solution for performing precise measurements with very low light power, allowing the study of living samples and delicate biological structures without damage. In this section, four key methods in quantum measurement are reviewed that have the greatest potential for application in sensitive biometry: 1. Measurement with entangled photons 2. Measurement with NOON modes 3. Measurement with squeezed light 4. Measurement with Fock states and single photons. Each of these methods is analyzed not only in terms of its specific physical principles, but also their advantages, limitations, and biological applications are examined with prominent experimental examples to clearly demonstrate their role in the development of quantum biometry technologies.

5.1. Comparison of measurement accuracy in quantum and classical

In biological measurements, one of the main challenges is the sensitivity of samples to light and the photodamage caused by high radiation intensity. In many classical measurements, there is no choice but to increase the signal-to-noise ratio, but this can lead to photochemical or thermal damage to biological tissues. This problem is especially acute in living, humid environments or with delicate cellular structures. Quantum measurement provides a new solution to this problem by using low-intensity but structured light. Two key categories of light sources are considered in this regard: 1. Very low-intensity photons (single photons or very weak pulses), 2. Quantum correlated photons (entangled or squeezed), which can extract precise information from the sample without the need for high power. However, even under optimal conditions, the signal-to-noise ratio is subject to fundamental quantum mechanical constraints. Classically, this constraint is expressed as the Standard Quantum Limit, which limits the measurement accuracy to statistical fluctuations in the photon count. To achieve accuracy beyond this limit, it is necessary to use quantum light sources with N-photon correlations, which theoretically can improve the accuracy by orders of magnitude $\sqrt{(1/N)}$. One of the key parameters in bioassays is the attenuation coefficient of the sample, which describes the degree to which light is absorbed or scattered by a biological material. Accurate evaluation of this coefficient is particularly important in tissue diagnostics, optical imaging, and the investigation of the optical response of cells. In

Biomedical Optics EXPRESS

the following, the achievable accuracy for estimating this coefficient within the framework of quantum mechanics is investigated.

The presence of a large unknown distortion can lead to non-optimal sampling of the field, reducing the effective measurement efficiency, which is equivalent to adding loss and further degrading achievable quantum enhancement. The precision for estimating attenuation coefficient in quantum mechanics can be written as Eq. (20):

$$\Delta A = \frac{\Delta^2 N}{\sqrt{M}\left(\partial \langle N\rangle / \partial A\right)}. \tag{20}$$

where M is the repetitions of measurements, $\Delta^2 N = \sqrt{\langle N^2\rangle - \langle N\rangle^2}$. By considering the classical statistical, the attenuation coefficient A is limited by the fundamental statistical fluctuations of the input beam for the signal-photons counting. In quantum mechanics, the coherent laser has the lowest noise. By considering the source as a classical coherent state, the variance of the attenuation coefficient expresses as Eq. (21):

$$\left\langle \Delta^2 \bar{N}\right\rangle = (1-A)^2\left[\left\langle \Delta^2 \bar{N}\right\rangle - \left\langle \bar{N}\right\rangle\right] + (1-A)\left\langle \bar{N}\right\rangle. \tag{21}$$

By employing $\partial \langle N\rangle / \partial A = N$ and $M = 1$, the variance of the attenuation coefficient is written as Eq. (22):

$$\Delta A = \sqrt{(1-A)}. \tag{22}$$

The radiation from a laser can usually be well described by a single-mode coherent state exhibiting Poissonian distribution. The probability of detecting n photons before passing the sample is $P(n) = e^{-\bar{N}}\bar{N}^n/n!$. Clearly, a highly attenuated laser pulse with very small $\bar{N}$ represents a good approximation of the single-photon Fock state. After passing the attenuated sample, the probability of detecting n photons can write as Poisson distribution as Eq. (23):

$$P(n) = e^{-\bar{N}(1-A)}[\bar{N}(1-A)]^n/n!. \tag{23}$$

Notice that the distribution of the photons number in one mode is thermal, whereas the total number in all modes obeys Poissonian distribution. For the Fock state, $|N\rangle$ as the probe, the attenuation due to the sample has a binomial distribution as Eq. (24):

$$p(n) = \begin{pmatrix} N \\ n \end{pmatrix}(1-A)^n A^{N-n}. \tag{24}$$

For the Fock state $\left\langle \Delta^2 N\right\rangle = 0$ and $M = 1$, so the attenuation coefficient A can written as Eq. (25):

$$\Delta A = \sqrt{(1-A)/A} \tag{25}$$

However, the attenuation coefficient is bound in precision by the shot-noise limit. Be comparing the attenuation coefficient on classical and quantum approaches, an improvement of $1/\sqrt{A}$ over the shot-noise limit is clear.

5.2. Quantum measurement with entangled photons

Quantum entanglement is one of the most fundamental properties of quantum mechanics, in which the states of two or more particles (such as photons) are related in such a way that measuring one immediately gives information about the other, even if they are spatially separated. In bio measuring methods based on entangled photons, this strong correlation is used to increase accuracy and reduce noise. In this case, one of the photons of the entangled pair interacts with

Biomedical Optics EXPRESS

the biological sample, while the other photon remains in the reference path. By simultaneously comparing the response of the two photons, very subtle changes in the optical properties of the sample (such as absorption, phase shift, scattering, etc.) can be extracted, even in conditions of high ambient noise or light attenuation. Since the information of the entire system is encoded in the correlation between the two photons, this method is very robust against optical loss, environmental changes, and complex cellular scattering. These properties make entangled photons a powerful tool for detecting structural or biomolecular differences in highly sensitive biological samples [86–90]. We will continue to study the work done in this field, including the study of light penetration in diluted DNA and thin layers by Motazedifard and Madani, the study of the preservation of entanglement in mouse brain tissue by Lotfipour et al., and others. Motazedifard and Madani employed the coincidence-count (CC) method to measure the transmittance of highly diluted rabbit- and human-DNA, methylene-blue (MB) as a disinfectant, and a thin-film multilayer at a near IR wavelength of 810 nm. They employed a frequency-entangled twin-photon beam and achieved an accuracy on the order of 0·01% due to the quantum correlation [91]. In 2024, Zhang and colleagues introduced an innovative and highly sensitive technique for examining single-layer cell cultures using entangled photon pairs. Their method (Fig. 6) shows promise for analyzing monolayer cell cultures and distinguishing between two types of cells as well as their host medium. They investigated the possibility of using polarization-entangled photon pairs to examine monolayer cultures of mammalian cells with a low polarization response. They conducted experiments to demonstrate the potential of this approach by distinguishing various cell cultures based on quantum state changes. Their findings indicate practical applications for characterizing biological samples [92].

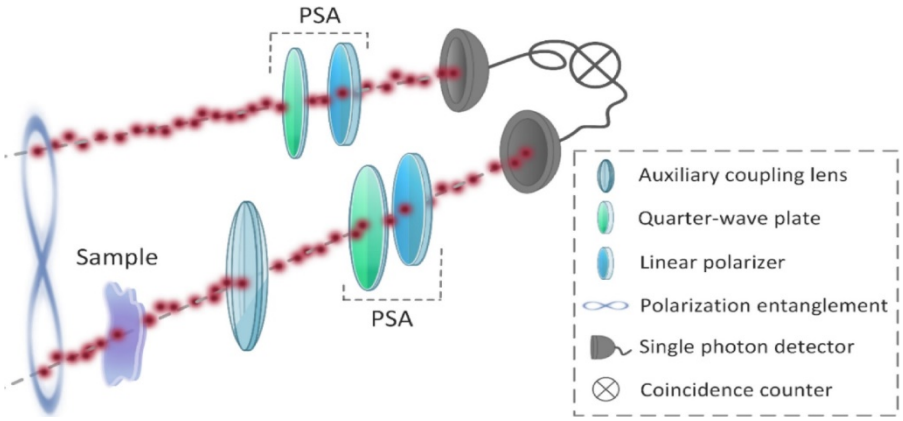


Fig. 6. Conceptual sketch of the optical setup used in the experiments conducted by Zhang and colleagues. Reproduced from ref. [92].

In a separate study conducted by Lotfipour and colleagues in the same year, they utilized quantum photon pairs generated through SPDC. This method involved creating pairs of photons in maximally entangled Bell states in the polarization degree of freedom. One set of entangled photons was directed towards rat brain tissue, and the state of the photons passing through the brain was observed. The researchers compared the preservation of the quantum correlation of the photon pairs in polarization by measuring the Bell parameter of the transmitted entangled photons. Their findings revealed a noticeable variation in the preservation of entanglement across different areas of the rat brain. It was found that the cortex tissue effectively maintained the correlation of the photons to a significant extent despite the scattering effect, while the inner regions, such as the amygdala, led to a decline in entanglement, resulting in the Bell parameter dropping to 1·31 [93].

Biomedical Optics EXPRESS

5.3. Quantum measurement with NOON states

NOON states are a special quantum state of light in which all photons are simultaneously in one of two paths of an interferometer. More precisely, in the NOON state with the number N photons either all photons are in the first arm, or all are in the second arm, and there is never any intermediate combination. These quantum states are extremely sensitive to the phase difference between the two arms, such that even very small changes in the phase of the light (which may be caused by changes in the refractive index, temperature, or concentration of a biological material) cause noticeable changes in the output interference pattern. Since the phase response of NOON modes is amplified by the N power, the measurement accuracy can be increased to several times the classical limit using a small number of photons. In biological applications, this property is very valuable, since very high measurement sensitivity can be achieved without increasing the light intensity - which may cause damage to the sample. For this reason, NOON modes are very useful for measuring the refractive index of biological fluids, the concentration of proteins, or monitoring biochemical reactions at the cellular and molecular scales. We will continue to study the work done, including measuring protein concentration with Mach-Zehnder interferometer in the Crespi study, tracking biochemical reactions such as sucrose hydrolysis, and other work in this field. In a well-known study by Crespi et al., a Mach-Zehnder interferometer was used to transmit a two-photon NOON state, with one arm containing a microfluidic channel. The researchers then employed a standard interferometric phase measurement to deduce the refractive index of the fluid in the channel. Measurements of the refractive index of a solution within a microfluidic device were then utilized to determine the protein concentration of the solution [94]. In 2021, Zheng Peng and colleagues presented a method for tracking the sucrose hydrolysis reaction in real time using two-photon coincidence measurements. The two-photon source is created using SPDC. Throughout the reaction, the kinetic parameters are determined by measuring the change in polarization of the photons in real time under very low-light conditions. Two-photon coincidence measurements offer higher SNRs and better robustness compared to single-photon counting measurements [95].

Yun Peng et al. introduced a novel approach for detecting photosensitive biomolecules without using labels in their paper published in 2023. To address the issue of external stray light impacting the detection outcome, they presented a microfiber quantum sensor designed for accurately measuring proteins using a two-photon NOON state. The utilization of the two-photon NOON state helps to mitigate the influence of classical interference fringes and enhance the sensor's stability. Changes in coincidence count enable the determination of biological sample concentration. In the case of bovine serum albumin concentration measurement, the quantum sensing system demonstrates a sensitivity of 0·2911 /(mg/mL) and a detection limit of 0·023 mg/mL. The recorded visibility stands at 85·2 ± 6·7%, which notably exceeds the visibility threshold required to surpass the standard quantum limit Vth=0·707, high-lighting the sensor's exceptional precision [96].

5.4. Quantum measurement with squeezed light

Squeezed light is a quantum state of light in which the quantum noise of one component of the electromagnetic field (such as phase or amplitude) is reduced and the noise of the other component is increased. If this noise reduction is properly tuned, the measurement accuracy can be increased beyond the shot-noise limit using the same classical optical power. The main advantage of squeezed light in biometry is that conventional high-intensity lasers can be used to generate the optical current, but by adding a squeezed component, the final sensitivity of the device can be significantly increased. This allows the detection of very small movements or mechano-optical changes, without the need for single-photon detectors. In biological applications, such as tracking nanoparticles within cells, or studying cytoplasmic viscosity, compressed light has the ability to separate the useful signal from ambient noise and increase the accuracy of

Biomedical Optics EXPRESS

imaging or measurement to a level that is not achievable with classical methods. As examples of the work done, we will examine Taylor's tracking of fat granules inside yeast cells with 42% noise reduction below the quantum limit, and sub-shot noise imaging with sensitive phase amplification [67,97].

In light of these advancements, Taylor et al. incorporated squeezed light into optical tweezers in order to monitor nanoscale particles below the quantum shot noise threshold. Their experimental results show that it is possible to surpass the quantum shot noise limit when making measurements on living systems. Quantum-correlated light with amplitude noise squeezed 75% below the vacuum level was utilized to conduct microrheology experiments within Saccharomyces cerevisiae yeast cells. Natural lipid granules were tracked in real time as they diffused through the cytoplasm, and the quantum noise limit was exceeded by 42%. The laser-based microparticle tracking method employed is compatible with non-classical light and is resistant to low-frequency interference, paving the way for a wide range of quantum-enhanced measurements in biology [67]. Eugene Knyazev et al. researched the measurement of absorption in 2019, demonstrating that accuracy can surpass the shot-noise limit through photon-number squeezing and correlations. They illustrated the potential solution to this issue as phase-sensitive amplification before detection. Additionally, they put forward a practical method for sub-shot-noise imaging that is tolerant to detection losses [97]. In 2023, Yanbo Lou et al. conducted a study in which they experimentally demonstrated an increase in quantum squeezing using phase-sensitive cascaded four-wave mixing (CFWM) processes. The intensity-difference squeezing (IDS) between the two outputs of the phase-sensitive CFWM processes was amplified to around 7·42 dB compared to IDS produced by the single four-wave mixing (FWM) process (approximately 3·31 or 4·01 dB). This enhancement resulted from the inherent interference nature of phase-sensitive CFWM processes and the increased gain from the two FWM processes. Furthermore, IDS levels generated by phase-sensitive CFWM processes at different internal-phase-locking points were measured, indicating the significant role of internal phase in IDS enhancement. This approach presents a novel means of enhancing the degree of IDS and may have potential applications in improving measurement precision in quantum metrology [98].

5.5. Quantum measurement with Fock states and single photons

In the Fock mode, there is a precise and constant number of photons in the light field (e.g., exactly one photon). This property allows the attenuation or scattering of light upon impact with the biological sample to directly affect the statistical distribution of the number of detected photons, which, with precise statistical modeling (e.g., with a binomial distribution), can be used to estimate the properties of the sample with high accuracy. In single-photon modes, the advantage is that the interaction between light and biological material can be observed discretely and countably, without relying on light intensity calibration or complex detectors. This approach is particularly useful for studying highly sensitive photoreceptors, such as retinal cells, or for distinguishing between healthy and cancerous tissues with high accuracy. Since in this method each photon carries independent information, it is possible to extract precise statistical properties of the sample with minimal optical power (and therefore without biological damage) by repeating measurements [99,100]. We will continue to study cases in this field, including one of the most famous examples in this field, namely measuring the quantum efficiency of retinal photoreceptor cells (rod cells). Phan et al. conducted a significant study on the interaction between a specialized light source that emits flashes with only one photon and the retinal rod cells of Xenopus laevis toads. Their research provided unequivocal evidence of the single-photon sensitivity of rod cells without relying on statistical modeling. Without the use of precalibrated detectors, they determined the quantum efficiencies and obtained a value of (29±4·7)% [101]. In other study conducted by Lotfipour and colleagues in the same year, they utilized the heralded single photons generated by the SPDC process to diagnosing cancer. In the approach, the measurement of

Biomedical Optics EXPRESS

light with precision beyond the shot-noise limit and near the ultimate quantum limit can be attained. The interaction of the heralded single photons with normal and malignant breast tissues announces the presence of its partner. Theoretically and experimentally, by comparing the measured attenuation coefficient of the normal and malignant tissues has been demonstrated using the heralded single photons [93].

The four main quantum measurement techniques introduced in this section, each exploiting the unique properties of quantum light, provide innovative avenues for precise and low-risk measurements in biological systems. The use of entangled photons, NOON states, compressed light, and single photons allows for measurements that go beyond classical limitations and with minimal damage to light-sensitive samples. These methods not only enable the study of biological processes at the nanometer scale, but also provide the infrastructure for the development of a new generation of quantum-based diagnostic and analytical tools in the life sciences. Combining these methods with emerging technologies such as microfluidics, integrated optics, and machine learning could provide researchers and clinicians with new perspectives for imaging, sensing, and disease diagnosis in the future.

6. Quantum materials for imaging

As previously mentioned, bioimaging is essential in both research and clinical environments, allowing for the observation and examination of biological processes, and ranging from individual cells to small animals. It is an invaluable tool for early disease detection and monitoring treatment effectiveness. There are two paths for quantum to enter bio-imaging, both of which seek to increase the accuracy and resolution of imaging. The first approach uses quantum lights as a tool to increase accuracy, which was discussed earlier. The second approach seeks to use quantum materials to improve image resolution.

Alongside quantum light sources used in biological imaging, quantum materials have several applications in biology, including imaging. These materials have distinctive properties, such as a high charge carrier density, large surface area, and significant interfacial area between the material and electrodes, which enhance electron transfer between the material and the sensing electrodes, making them excellent candidates for use in biosensors [17]. For instance, 2D quantum materials have been extensively studied for their potential in biosensors and bioimaging technologies. Graphene-based sensors, in particular, have shown enhanced sensitivity, mechanical strength, and biocompatibility compared to conventional materials like silicon. This heightened sensitivity results from the atomic thickness and large surface area-to-volume ratios of 2D materials, allowing most atoms to interact directly with analytes [17]. These properties facilitate the creation of flexible, durable, and commercially feasible real-time biosensing devices. Bioimaging is another field of quantum materials application. Among quantum materials, graphene quantum dots (GQDs) and nanographene, in particular, show great promise for next-gen bioimaging devices, thanks to their low toxicity, strong photoluminescence, magnetic resonance signatures, and adjustable fluorescence. Compared to traditional semiconductor quantum dots, they offer benefits like reduced toxicity, better biocompatibility, greater chemical stability, and improved solubility [17]. Recently, Abdul Rasheed and co-workers [102] reviewed the applications of graphene quantum dots for biosensing and bioimaging. As they mentioned GQDs are recognized for their ability to track therapeutic responses and distribution in vivo due to their exceptional photostability and versatile photoluminescence properties. They are commonly used as bioimaging agents for visualizing tumors alongside targeted drug delivery. Recent research highlights the potential of Graphene Quantum Dots (GQDs) for near-infrared (NIR) and magnetic resonance (MR) imaging. These distinctive characteristics have prompted researchers to explore GQDs for cancer cell imaging, including HeLa cells, MG-63 cells, and MCF-7 cells, among others. This imaging technique utilizes visible and near-IR radiation to monitor the distribution of various analyte molecules within animal cells and tissues. The adaptability of GQDs allows for their modification,

Biomedical Optics EXPRESS

making them suitable as imaging probes for cell nuclei. Using structural modification of GQDs, they exhibited highly positive zeta potentials, enabling them to pass through cell membranes and bind directly to histones in the cell nuclei. Given their minimal cytotoxicity, these structures present a promising option as stable fluorescent agents for in vitro imaging. Due to their high solubility in water, these zero-dimensional structures can easily enter cells without requiring additional targeting molecules. Modifying their photoluminescence properties can enhance their use alongside other fluorescent probes for cellular process analysis. In two-photon confocal imaging, HeLa cells were treated with GQDs and exposed to an 800 nm laser. The images confirmed cellular uptake and strong fluorescence, validating the GQDs for long-term two-photon fluorescence microscopy. In another approach, nitrogen-doped GQDs (N-GQDs) were created by treating dimethyl formaldehyde with graphene oxide. Their two-photon fluorescence was explored for efficient cellular and deep tissue imaging. The good biocompatibility and exceptional photostability of N-GQDs support long-term two-photon fluorescence imaging in biological tissues. The synthesized N-GQDs exhibited blue-green fluorescence, and their fluorescence images revealed penetration into the cytoplasm but not the nuclei of HeLa cells. Wang et al. [103] developed N–B-GQDs for near-infrared (NIR-II) bioimaging, which were GQDs doped with nitrogen and boron. The N–B-GQDs exhibited NIR-II photoluminescence in the 950–1100 nm range when excited at 808 nm. The authors suggested that the nitrogen and boron doping introduced vacancy defects, which caused the emission peak to shift into the NIR-II range. They first confirmed that N–B-GQDs were non-toxic to three different cell lines, and then demonstrated the in vivo photoluminescence properties of these NIR-II fluorophores through a series of images taken after intravenous injection in nude athymic mice over 120 minutes (Fig. 7).

Rai et al. [104] demonstrated that functionalized WS_2 quantum dots (QDs) can serve as fluorescent nanoprobes for in-vivo bioimaging. They highlighted that the strong fluorescence and high photostability of inorganic QDs make them superior to organic dyes, which are susceptible to photobleaching, for biomedical imaging applications. However, previous studies have indicated that the effective use of inorganic QDs depends on their ability to remain fluorescent and stably dispersed in water and other biological fluids across a broad pH range. This study focuses on the impact of pH (ranging from 1·0 to 13·0) on the photophysical properties of functionalized tungsten disulfide QDs (f-WS_2-QDs), which were synthesized using a simple, eco-friendly, one-step hydrothermal method. Experimental results indicate that the fluorescence properties of as-synthesized f-WS_2-QDs remain exceptionally stable across a broad range of acidic to basic conditions. The stability of their photoluminescence and their dispersion in aqueous solutions can be attributed to the various functional groups on the QDs' surface, which contribute to surface passivation during hydrothermal synthesis. This passivation enhances both the solubility and the stable fluorescence of the QDs in water. Additionally, as a proof of concept, they have demonstrated the potential of f-WS_2-QDs as a fluorescent probe for high-contrast in vivo imaging of Drosophila third instar larvae. This study provides valuable insights for the development of pH-universal inorganic QDs for biological applications. For the fluorescence study, 40 μL/mL treated late third instar larval gut tissues were analyzed. The results show significant uptake of f-WS_2-QDs, particularly in the gut (Fig. 8). Consequently, this self-activated fluorescence compound proves to be effective for bioimaging of the gut and other tissues in Drosophila third instar larvae.

Nanodiamonds are another type of quantum material used in biological imaging. Leveraging quantum systems, particularly the strong sensitivity of atomic spin states to physical factors, allows for the detection of even very weak signals, showcasing the key benefits of quantum sensing. Among different technologies, the methods for detecting and polarizing the spin states of diamond's negatively charged nitrogen-vacancy (NV) centers are simple and effective at ambient conditions (like room temperature), offering notable advantages from several viewpoints. As a result, this technique has emerged as one of the most promising options for quantum

Biomedical Optics EXPRESS

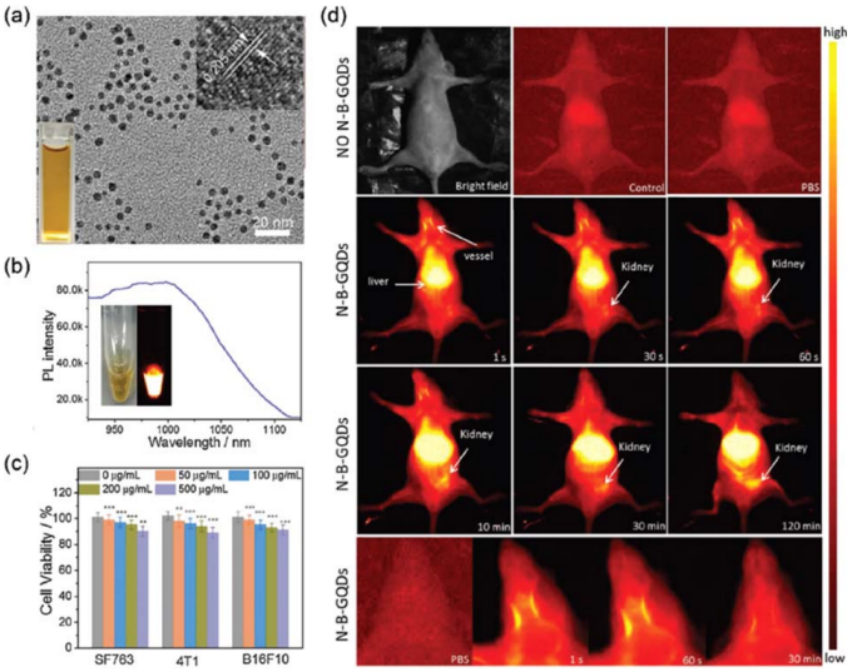


Fig. 7. Nitrogen and boron dual-doped GQDs for NIR-II bioimaging. (a) TEM image showing the monodisperse particles (b) photoluminescence spectrum of N–B-GQDs exhibiting NIR-II emission when excited with an 808 nm laser source. The insets display an optical image a photoluminescence image of N–B-GQDs in aqueous solution. (c) In vitro cytotoxicity study of N–B-GQDs performed by assessing the viability of SF763, 4T1, and B16F10 cells 72 h after incubation with N–B-GQDs. (d) In vivo NIR-II imaging of live mice. Adapted with permission from Ref. [103]. Copyright 2019 Elsevier.

sensing in recent years [17]. Despite these advancements, the high refractive index of diamond results in significant total reflection during measurements, which significantly reduces the intensity of emitted fluorescence. This causes a low SNR in the system, greatly impacting the magnetometer's performance. As a result, boosting fluorescence emission intensity is a key approach to improving quantum sensing with NV centers [17]. Studying biological processes in real-time is challenging because it demands accurate measurements while reducing the impact on the system being observed. This involves not only considering the space taken up by instruments but, more importantly, minimizing any disruption to the conditions in which the system operates. For instance, illuminating a sample too strongly may cause the sample to heat due to absorption, although the increased flux would provide per se a better SNR. Liu et al. investigated novel uses of nanodiamonds (NDs) containing silicon-vacancy centers (SiV), which were synthesized using a high-pressure high-temperature (HPHT) method without metal catalysts. Their NDs were coated with a polypeptide biopolymer to enhance cellular uptake. These NDs with SiV exhibit exceptional optical properties, including high photostability and narrow near-infrared emission. This study is the first to demonstrate that NDs with SiV enable dual-color live-cell imaging and intracellular tracking. Additionally, it explores intracellular thermometry and addresses challenges related to SiV atomic defects in NDs for the first time. These nanoemitters open new possibilities for live-cell bioimaging, diagnostics (using SiV as a nanoscale thermometer), and theranostic applications, such as drug delivery. NDSiV-polymer nanoparticles have been evaluated for intracellular thermometry in both fixed and live A549 cells, using fixed cells as a control to limit the movement of NDs compared to live cells (Fig. 9(a)).

Biomedical Optics EXPRESS

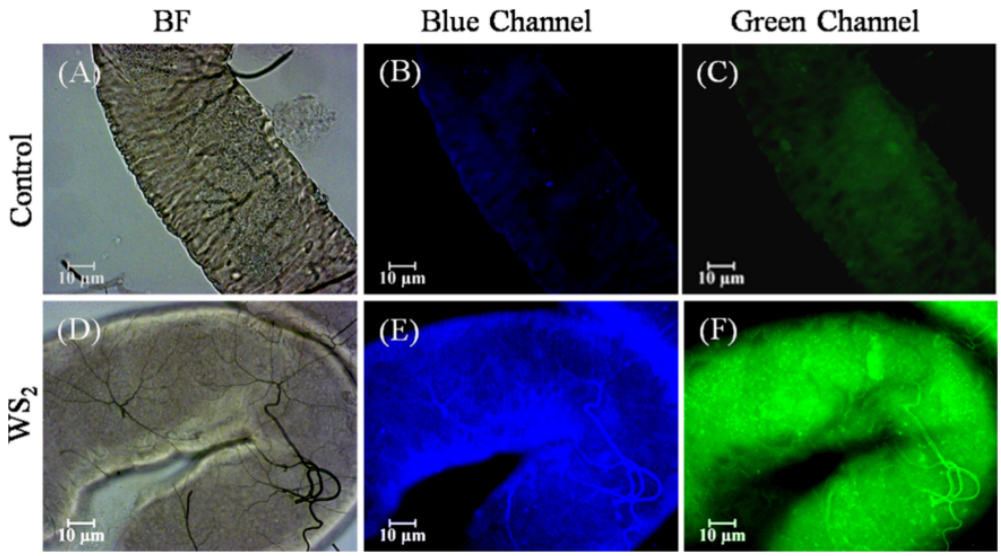


Fig. 8. Fluorescence images obtained at 20X, representing the fluorescence enrichment of compound *f*-WS_2-QDs in the gut tissues of Drosophila third instar larvae. Upper panels (B, C) exhibit no fluorescence considered as control. Lower panel (E, F) demonstrates fluorescence in gut tissues of Drosophila third instar larvae. (A and D) shows BF (Bright Field) images of their respective panel. Reproduced with permission from Ref. [104]. Copyright © 2023 American Chemical Society.

We explored the impact of the cellular environment on ND-SiV fluorescence, as even minimal cellular autofluorescence can interfere with the SiV spectra and affect thermometry accuracy. Inside cells, the NDSiV-polymer signals typically come from ND clusters within intracellular vesicles. Unfortunately, all NDSiV-polymer spots tested within cells exhibit zero phono line (ZPL) peaks above 738·2 nm at 25 °C, making them unsuitable for precise thermometry. All the measured locations show red shifts in the ZPL peak positions. In one of the measured spots of NDSiV-polymer in living cells, a red shift of approximately ~0·06218 nm (average of seven measurements) was observed when the temperature increased from 25°C to 37°C. Using ND-SiV for live-cell thermometry not only requires sensing but also the ability to track the NDs. As an initial attempt, we tracked 135 individual NDSiV polymer spots within living HeLa cells over 90 minutes, with refocusing intervals of 40 seconds. A representative trajectory of one NDSiV spot is shown in Fig. 9(c). The tracking measurements are carried out using the fluorescence intensities of NDSiV-polymer during the experiments. These fluorescence intensities of the tracked NDSiV-polymer remain fairly consistent (Fig. 9(c)) with minimal fluctuations. Any fluctuations observed may be due to rapid diffusion away from the focal point of the objective or rotational movement caused by varying excitation efficiencies during tracking. Additional tracked NDs with representative trajectories and intensities are shown in. The presence of SiV is confirmed through spectral measurements. No significant decrease in fluorescence intensities is seen, allowing NDSiV-polymer to be used for long-term cellular tracking. We have previously reported live-cell dual-color imaging, thermometry, and tracking applications using NDs that contain only SiV, without any other color centers, produced by the improved metal-catalyst free HPHT method. This approach yields NIR emitters with a single, sharp emission signal. These ND-SiV particles are coated with a biopolymer derived from proteins, providing them with colloidal stability in water, buffers, and cell media. Key features of these nanoemitters include NIR fluorescence, a sharp ZPL, and excellent fluorescence stability, making them suitable for

Biomedical Optics EXPRESS

imaging and tracking in living cells. For the first time, HPHT ND-SiV have been successfully used in dual-color imaging and tracking experiments lasting up to 90 minutes inside living cells without photobleaching. Additionally, thermometry with small ND-SiV in water and cells is explored for the first time, revealing a novel ZPL shift in response to heat. We propose that ND-SiV holds significant potential as a tool for intracellular imaging, all-optical thermometry, and tracking, making them valuable for biological research. However, further in-depth and multidimensional studies are still needed to fully understand thermometry with ND-SiV. Since nanodiamonds can also serve as drug delivery agents, the combined properties of the ND-SiV system open up possibilities for theranostic applications [105].

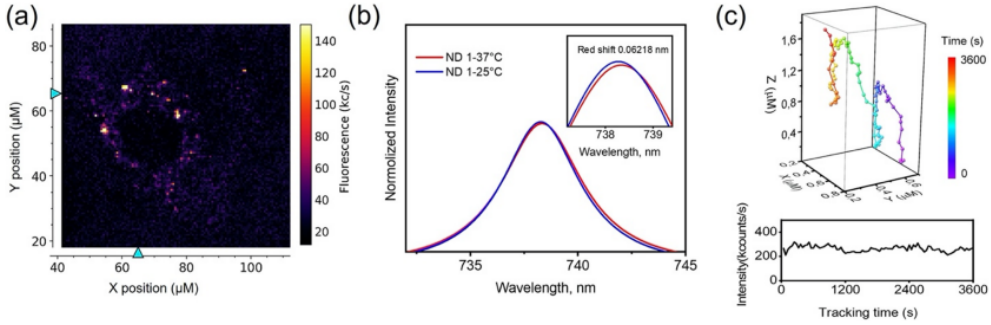


Fig. 9. NDSiV-polymer for living cell thermometry and intracellular tracking. (a) Custom-built confocal image of a living A549 cell with uptaken NDSiV-polymer nanoparticles. (b) Position of ZPL peaks of NDSiV-polymer at 25 and 37 °C. (c) Trajectory of NDSiV-polymer tracked in intracellular space [105].

7. Conclusion

Quantum technology, which leverages various quantum phenomena like quantum coherence, squeezing, entanglement, interference, and correlation, has recently attracted considerable attention. There is also an increasing interest in investigating the connection between quantum research and biology. Scientists have highlighted the importance of quantum technology for advancing biological studies. This article provides an overview of the potential applications of quantum technology in biology and medicine. It was found that quantum technology has various applications in biology, with quantum imaging, sensing, measurement, and spectroscopy being particularly crucial. For example, quantum metrology, which utilizes quantum light sources, devices, and protocols, can play a crucial role in enhancing imaging accuracy and resolution by detecting changes at quantum scales in biological systems. It also examines the current opportunities and challenges associated with advanced quantum biological imaging methods and materials. Finally, the applications of quantum materials in biological imaging were reviewed.

Disclosures. The authors declare no conflicts of interest.

Data availability. No data were generated or analyzed in the presented research.

References

1. C. A. Casacio, L. S. Madsen, A. Terrasson, *et al.*, "Quantum-enhanced nonlinear microscopy," Nature **594**(7862), 201–206 (2021).
2. J. Park, D. J. Brady, G. Zheng, *et al.*, "Review of bio-optical imaging systems with a high space-bandwidth product," Adv Photonics **3**(04), 044001 (2021).
3. M. Berg, N. Holroyd, and C. Walsh, "Challenges and opportunities of integrating imaging and mathematical modeling to interrogate biological processes," The International Journal of Biochemistry & Cell Biology **146**, 106195 (2022).
4. S. Vernekar and J. Xavier, "Quantum correlation enhanced optical imaging,"

Biomedical Optics EXPRESS

5. Y. Zhang, Z. He, X. Tong, *et al.*, "Quantum imaging of biological organisms through spatial and polarization entanglement," Sci. Adv. **10**(10), eadk1495 (2024).
6. R. Chatterjee, V. S. Bhat, K. Bajar, *et al.*, "Multifold enhancement of quantum SNR by using an EMCCD as a photon number resolving device," Optica Quantum **2**(3), 156–164 (2024).
7. H. Defienne, B. Ndagano, A. Lyons, *et al.*, "Polarization entanglement-enabled quantum holography," Nat. Phys. **17**(5), 591–597 (2021).
8. P.-A. Moreau, E. Toninelli, T. Gregory, *et al.*, "Imaging with quantum states of light," Nat. Rev. Phys. **1**(6), 367–380 (2019).
9. F. Li, T. Li, M. O. Scully, *et al.*, "Quantum advantage with seeded squeezed light for absorption measurement," Phys. Rev. Appl. **15**(4), 044030 (2021).
10. M. Kaur and M. Singh, "Quantum imaging of a polarisation sensitive phase pattern with hyper-entangled photons," Sci. Rep. **11**(1), 23636 (2021).
11. A. Saxena, M. Kaur, V. Devrari, *et al.*, "Quantum ghost imaging of a transparent polarisation sensitive phase pattern," Sci. Rep. **12**(1), 21105 (2022).
12. R. Tenne, U. Rossman, B. Rephael, *et al.*, "Super-resolution enhancement by quantum image scanning microscopy," Nat. Photonics **13**(2), 116–122 (2019).
13. E. Losero, I. Ruo-Berchera, A. Meda, *et al.*, "Quantum differential ghost microscopy," Phys. Rev. A **100**(6), 063818 (2019).
14. Inna Kviatkovsky, Helen M. Chrzanowski, Ellen G. Avery, *et al.*, "Microscopy with undetected photons in the mid-infrared," Sci. Adv. **6**(42), eabd0264 (2020).
15. Z. He, L. S. Madsen, A. Terrasso, *et al.*, "Quantum microscopy of cells at the Heisenberg limit," Nat. Commun. **14**(1), 2441 (2023).
16. R. Schirhagl, K. Chang, M. Loretz, *et al.*, "Nitrogen-vacancy centers in diamond: nanoscale sensors for physics and biology," Annu. Rev. Phys. Chem. **65**(1), 83–105 (2014).
17. M. Modayil Korah, T. Nori, S. Tongay, *et al.*, "Harnessing biological applications of quantum materials: opportunities and precautions," J. Mater. Chem. C **8**(31), 10498–10525 (2020).
18. X. Yue, H. Wu, J. Wang, *et al.*, "Quantum super-resolution imaging: a review and perspective," Nanophotonics **14**(11), 1961–1974 (2025).
19. H. Defienne, W. P. Bowen, M. Chekhova, *et al.*, "Advances in quantum imaging," Nat. Photonics **18**(10), 1024–1036 (2024).
20. E. Moreva, V. Cimini, I. Gianani, *et al.*, "Quantum photonics sensing in biosystems," APL Photonics **10**(1), 010902 (2025).
21. C. Couteau, "Spontaneous parametric down-conversion," Contemp. Phys. **59**(3), 291–304 (2018).
22. S. Karan, S. Aarav, H. Bharadhwaj, *et al.*, "Phase matching in β-barium borate crystals for spontaneous parametric down-conversion," J. Opt. **22**(8), 083501 (2020).
23. L.-J. Kong, Y. Sun, F. Zhang, *et al.*, "High-dimensional entanglement-enabled holography," Phys. Rev. Lett. **130**(5), 053602 (2023).
24. D. O'Connor, *Time-correlated single photon counting* (Academic press 2012).
25. M. D'Angelo, M. V. Chekhova, and Y. Shih, "Two-photon diffraction and quantum lithography," Phys. Rev. Lett. **87**(1), 013602 (2001).
26. L. Sansoni, F. Sciarrino, G. Vallone, *et al.*, "Polarization entangled state measurement on a chip," Phys. Rev. Lett. **105**(20), 200503 (2010).
27. P. G. Kwiat, E. Waks, A. G. White, *et al.*, "Ultrabright source of polarization-entangled photons," Phys. Rev. A **60**(2), R773–R776 (1999).
28. F. Anders, A. Idel, P. Feldmann, *et al.*, "Momentum entanglement for atom interferometry," Phys. Rev. Lett. **127**(14), 140402 (2021).
29. B. Hiesmayr, M. De Dood, and W. Löffler, "Observation of four-photon orbital angular momentum entanglement," Phys. Rev. Lett. **116**(7), 073601 (2016).
30. M. D. Reid, P. D. Drummond, W. P. Bowen, *et al.*, "Colloquium: the Einstein-Podolsky-Rosen paradox: from concepts to applications," Rev. Mod. Phys. **81**(4), 1727–1751 (2009).
31. Z.-S. Yuan, X.-H. Bao, C.-Y. Lu, *et al.*, "Entangled photons and quantum communication," Phys. Rep. **497**(1), 1–40 (2010).
32. G. Arun and V. Mishra, "A review on quantum computing and communication," in *2014 2nd International Conference On Emerging Technology Trends In Electronics, Communication And Networking* (2014). IEEE.
33. C. Moodley and A. Forbes, "All-digital quantum ghost imaging: tutorial," J. Opt. Soc. Am. B **40**(12), 3073–3095 (2023).
34. S.N. Ahmed, "Physics and Engineering of Radiation Detection," (2nd ed.), Elsevier (2015).
35. S. Zhang, F. Wang, X. Wu, *et al.*, "MTF measurement by slanted-edge method based on improved Zernike moments," Sensors **23**(1), 509 (2023).
36. B.-Y. Go, C. Lee, and K.-G. Lee, "Theoretical studies on quantum imaging with time-integrated single-photon detection under realistic experimental conditions," Sci. Rep. **12**(1), 5338 (2022).
37. G. Brida, M. V. Chekhova, G. A. Fornaro, *et al.*, "Systematic analysis of signal-to-noise ratio in bipartite ghost imaging with classical and quantum light," Phys. Rev. A **83**(6), 063807 (2011).

Biomedical Optics EXPRESS

38. C. Lupo, "Subwavelength quantum imaging with noisy detectors," Phys. Rev. A **101**(2), 022323 (2020).
39. B. I. Erkmen and J. H. Shapiro, "Signal-to-noise ratio of Gaussian-state ghost imaging," Phys. Rev. A **79**(2), 023833 (2009).
40. M. Genovese, "Real applications of quantum imaging," J. Opt. **18**(7), 073002 (2016).
41. T. Gregory, P.-A. Moreau, E. Toninelli, *et al.*, "Imaging through noise with quantum illumination," Sci. Adv. **6**(6), eaay2652 (2020).
42. E. Toninelli, P.-A. Moreau, T. Gregory, *et al.*, "Resolution-enhanced quantum imaging by centroid estimation of biphotons," Optica **6**(3), 347–353 (2019).
43. M. Unternährer, *et al.*, "Super-resolution quantum imaging at the Heisenberg limit," Optica **5**(9), 1150–1154 (2018).
44. M. A. Taylor and W. P. Bowen, "Quantum metrology and its application in biology," Phys. Rep. **615**, 1–59 (2016).
45. S. Vernekar and J. Xavier, "Quantum Correlation Enhanced Optical Imaging," Quantum Beam Sci. **8**(3), 19 (2024).
46. Y. Zhang, A. Sit, F. Bouchard, *et al.*, "Interaction-free ghost-imaging of structured objects," Opt. Express **27**(3), 2212–2224 (2019).
47. T. B. Pittman, Y. H. Shih, D. V. Strekalov, *et al.*, "Optical imaging by means of two-photon quantum entanglement," Phys. Rev. A **52**(5), R3429–R3432 (1995).
48. P. Moreau, E. Toninelli, T. Gregory, *et al.*, "Ghost imaging using optical correlations," Laser Photonics Rev. **12**(1), 1700143 (2018).
49. A. Gatti, E. Brambilla, and L. Lugiato, "Quantum imaging," Prog. Opt. **51**, 251–348 (2008).
50. P. A. Morris, R. S. Aspden, J. E. C. Bell, *et al.*, "Imaging with a small number of photons," Nat. Commun. **6**(1), 5913 (2015).
51. R. S. Aspden, N. R. Gemmell, P. A. Morris, *et al.*, "Photon-sparse microscopy: visible light imaging using infrared illumination," Optica **2**(12), 1049–1052 (2015).
52. G. Brida, M. Genovese, and I. Ruo Berchera, "Experimental realization of sub-shot-noise quantum imaging," Nat. Photonics **4**(4), 227–230 (2010).
53. N. Samantaray, I. Ruo-Berchera, A. Meda, *et al.*, "Realization of the first sub-shot-noise wide field microscope," Light: Sci. Appl. **6**(7), e17005 (2017).
54. I. Ruo-Berchera, *et al.*, "Improving resolution-sensitivity trade off in sub-shot noise quantum imaging," Appl. Phys. Lett. **116**(21), 214001 (2020).
55. X. Zou, L. J. Wang, and L. Mandel, "Induced coherence and indistinguishability in optical interference," Phys. Rev. Lett. **67**(3), 318–321 (1991).
56. G. Barreto Lemos, M. Lahiri, S. Ramelow, *et al.*, "Quantum imaging and metrology with undetected photons: tutorial," J. Opt. Soc. Am. B **39**(8), 2200–2228 (2022).
57. S. Töpfer, M. Gilaberte Basset, J. Fuenzalida, *et al.*, "Quantum holography with undetected light," Sci. Adv. **8**(2), eabl4301 (2022).
58. G. B. Lemos, V. Borish, G. D. Cole, *et al.*, "Quantum imaging with undetected photons," Nature **512**(7515), 409–412 (2014).
59. D. A. Kalashnikov, A. V. Paterova, S. P. Kulik, *et al.*, "Infrared spectroscopy with visible light," Nat. Photonics **10**(2), 98–101 (2016).
60. A. Zeilinger, Sven Ramelow, Radek Lapkiewicz, *et al.*, Quantum imaging with undetected photons,: US Patents, US9557262B2.
61. A. Búzás, E. K. Wolff, M. G. Benedict, *et al.*, "Biological microscopy with undetected photons," IEEE Access **8**, 107539–107548 (2020).
62. A. G. White, J. R. Mitchell, O. Nairz, *et al.*, ""Interaction-free" imaging," Phys. Rev. A **58**(1), 605–613 (1998).
63. S. Ahmadi, E. Saglamyurek, S. Barzanjeh, *et al.*, "High-contrast interaction-free quantum imaging method," Phys. Rev. A **107**(3), 032611 (2023).
64. A. M. Pălici, T.-A. Isdrailă, S. Ataman, *et al.*, "Interaction-free imaging of multipixel objects," Phys. Rev. A **105**(1), 013529 (2022).
65. Yingwen Zhang, Lu Gao, Alicia Sit, *et al.*, "Interaction-free quantum imaging," in *Nanoscale Imaging, Sensing, and Actuation for Biomedical Applications XVII*. 2020. SPIE.
66. Y. Yang, H. Liang, X. Xu, *et al.*, "Interaction-free, single-pixel quantum imaging with undetected photons," npj Quantum Inf. **9**(1), 2 (2023).
67. M. A. Taylor, J. Janousek, V. Daria, *et al.*, "Biological measurement beyond the quantum limit," Nat. Photonics **7**(3), 229–233 (2013).
68. M. Lelek, M. T. Gyparaki, G. Beliu, *et al.*, "Single-molecule localization microscopy," Nat. Rev. Methods Primers **1**(1), 39 (2021).
69. I. Kviatkovsky, H. M. Chrzanowski, and S. J. O. E. Ramelow, "Mid-infrared microscopy via position correlations of undetected photons," Opt. Express **30**(4), 5916–5925 (2022).
70. C. Torre, "Microscopy with Quantum States of Light," Doctoral Thesis, 2023.
71. C. Torre, A. McMillan, J. Monroy-Ruz, *et al.*, "Sub-μ m axial precision depth imaging with entangled two-color Hong-Ou-Mandel microscopy," Phys. Rev. A **108**(2), 023726 (2023).
72. B. Ndagano, H. Defienne, D. Branford, *et al.*, "Quantum microscopy based on Hong–Ou–Mandel interference," Nat. Photonics **16**(5), 384–389 (2022).
73. T. Ono, R. Okamoto, and S. Takeuchi, "An entanglement-enhanced microscope," Nat. Commun. **4**(1), 2426 (2013).

Biomedical Optics EXPRESS

74. D. S. Simon and A.V. Sergienko, "The correlation confocal microscope," Opt. Express **18**(10), 9765–9779 (2010).
75. D. S. Simon and A. V. Sergienko, "Twin-photon confocal microscopy," Opt. Express **18**(21), 22147–22157 (2010).
76. A. Terrasson, N. P. Mauranyapin, C. A. Casacio, *et al.*, "Fast biological imaging with quantum-enhanced Raman microscopy," Opt. Express **32**(21), 36193–36206 (2024).
77. R. B. de Andrade, H. Kerdoncuff, K. Berg-Sørensen, *et al.*, "Quantum-enhanced continuous-wave stimulated Raman scattering spectroscopy," Optica **7**(5), 470–475 (2020).
78. B. Huang, W. Wang, M. Bates, *et al.*, "Three-dimensional super-resolution imaging by stochastic optical reconstruction microscopy," Sience **319**(5864), 810–813 (2008).
79. W. P. Bowen, H. M. Chrzanowski, D. Oron, *et al.*, "Quantum light microscopy," Contemp. Phys. **64**(3), 169–193 (2023).
80. D.-I. Lee and T. Goodson, "Entangled photon absorption in an organic porphyrin dendrimer," J. Phys. Chem. B **110**(51), 25582–25585 (2006).
81. A. R. Guzman, M. R. Harpham, Ö. Süzer, *et al.*, "Spatial control of entangled two-photon absorption with organic chromophores," J. Am. Chem. Soc. **132**(23), 7840–7841 (2010).
82. B. E. A. Saleh, M. C. Teich, and A. V. Sergienko, "Wolf equations for two-photon light," Phys. Rev. Lett. **94**(22), 223601 (2005).
83. Y. Israel, S. Rosen, and Y. Silberberg, "Supersensitive polarization microscopy using NOON states of light," Phys. Rev. Lett. **112**(10), 103604 (2014).
84. M. A. Taylor, J. Janousek, V. Daria, *et al.*, "Subdiffraction-limited quantum imaging within a living cell," Phys. Rev. X **4**(1), 011017 (2014).
85. Gil Triginer Garces, Helen M. Chrzanowski, Shakib Daryanoosh, *et al.*, "Quantum-enhanced stimulated emission detection for label-free microscopy," Appl. Phys. Lett. **117**(2), 024002 (2020).
86. H. Lotfipour, H. Sobhani, and M. Khodabandeh, "Quantum diagnosis of cancer with heralded single photons," Laser Phys. Lett. **19**(10), 105603 (2022).
87. L. Shi, E. J. Galvez, and R. R. Alfano, "Photon entanglement through brain tissue," Sci. Rep. **6**(1), 37714 (2016).
88. E. Galvez, L. Shi, B. Khajavi, *et al.*, "Transmission of Polarization-Entangled Photons Through Brain Tissue," Frontiers in Optics. 2017. OSA Technical Digest.
89. S. Mamani, L. Shi, T. Ahmed, *et al.*, "Transmission of classically entangled beams through mouse brain tissue," J. Biophotonics **11**(12), e201800096 (2018).
90. S. Mamani, L. Shi, D. Nolan, *et al.*, "Majorana vortex photons a form of entangled photons propagation through brain tissue," J. Biophotonics **12**(10), e201900036 (2019).
91. A. Motazedifard and S. A. Madani, "High-precision quantum transmittometry of DNA and methylene-blue using a frequency-entangled twin-photon beam in type-I SPDC," OSA Continuum **4**(3), 1049–1069 (2021).
92. L. Zhang, V. R. Besaga, P. Rühl, *et al.*, "Probing polarization response of monolayer cell cultures with entangled photon pairs," J. Biophotonics **2024**, 202400018 (2024).
93. H. Lotfipour, N. S. Vayaghan, M. Hafezi, *et al.*, "Quantum investigation: propagation of entangled photons through cortex tissue," Indian J. Phys. **99**(1), 25–31 (2025).
94. A. Crespi, M. Lobino, J. C. F. Matthews, *et al.*, "Measuring protein concentration with entangled photons," Appl. Phys. Lett. **100**(23), 233704 (2012).
95. Z. Peng, Z. Zhou, T. Li, *et al.*, "Real-time monitoring of the sucrose hydrolysis process based on two-photon coincidence measurements," Biomed. Opt. Express **12**(10), 6590–6600 (2021).
96. Y. Peng and Y. Zhao, "Microfiber quantum sensors for protein measurement with quantum N00N state," Sensors and Actuators B: Chemical **383**, 133616 (2023).
97. E. Knyazev, F. Y. Khalili, and M. V. Chekhova, "Overcoming inefficient detection in sub-shot-noise absorption measurement and imaging," Opt. Express **27**(6), 7868–7885 (2019).
98. Y. Lou, Y. Chen, J. Wang, *et al.*, "Quantum squeezing enhancement based on phase-sensitive cascaded four-wave mixing processes," Sci. China Phys. Mech. Astron. **66**(5), 250311 (2023).
99. D. A. Baylor, T. D. Lamb, and K.-W. Yau, "Responses of retinal rods to single photons," The Journal of Physiology **288**(1), 613–634 (1979).
100. F. Rieke and D. A. Baylor, "Single-photon detection by rod cells of the retina," Rev. Mod. Phys. **70**(3), 1027–1036 (1998).
101. N. M. Phan, M. F. Cheng, D. A. Bessarab, *et al.*, "Interaction of fixed number of photons with retinal rod cells," Phys. Rev. Lett. **112**(21), 213601 (2014).
102. P. A. Rasheed, M. Ankitha, V. K. Pillai, *et al.*, "Graphene quantum dots for biosensing and bioimaging," RSC Adv. **14**(23), 16001–16023 (2024).
103. H. Wang, Q. Mu, K. Wang, *et al.*, "Nitrogen and boron dual-doped graphene quantum dots for near-infrared second window imaging and photothermal therapy," Applied Materials Today **14**, 108–117 (2019).
104. S. Rai, V. K. Singh, B. S. Chauhan, *et al.*, "Functionalized WS_2 quantum dots as fluorescent nanoprobes for in vivo bioimaging," ACS Appl. Nano Mater. **6**(19), 17657–17667 (2023).
105. W. Liu, M. N. A. Alam, Y. Liu, *et al.*, "Silicon-vacancy nanodiamonds as high performance near-infrared emitters for live-cell dual-color imaging and thermometry," Nano Lett. **22**(7), 2881–2888 (2022).